2018

Sheeting joints and polygonal patterns in the Navajo Sandstone, southern Utah: Controlled by rock fabric, tectonic joints, buckling, and gullying

David B. Loope
University of Nebraska, Lincoln, dloope1@unl.edu

Caroline M. Burberry
University of Nebraska - Lincoln, cburberry2@unl.edu

Research Paper

GEOSPHERE

GEOSPHERE, v. 14, no. 4

https://doi.org/10.1130/GES01614.1

14 figures; 1 table

CORRESPONDENCE: dloope1@unl.edu

CITATION: Loope, D.B., and Burberry, C.M., 2018, Sheeting joints and polygonal patterns in the Navajo Sandstone, southern Utah: Controlled by rock fabric, tectonic joints, buckling, and gullying: Geosphere, v. 14, no. 4, https://doi.org/10.1130/GES01614.1.

Science Editor: Raymond M. Russo

Received 13 September 2017
Revision received 13 March 2018
Accepted 2 May 2018

Sheeting joints and polygonal patterns in the Navajo Sandstone, southern Utah: Controlled by rock fabric, tectonic joints, buckling, and gullying

David B. Loope and Caroline M. Burberry

Department of Earth and Atmospheric Sciences, University of Nebraska, Lincoln, Nebraska 68588, USA

ABSTRACT

Sheeting joints are ubiquitous in outcrops of the Navajo Sandstone on the west-central Colorado Plateau, USA. As in granitic terrains, these are opening-mode fractures and form parallel to land surfaces. In our study areas in south-central Utah, liquefaction during Jurassic seismic events destroyed stratification in large volumes of eolian sediment, and first-order sheeting joints are now preferentially forming in these structureless (isotropic) sandstones. Vertical cross-joints abut the land-surface-parallel sheeting joints, segmenting broad (tens of meters) rock sheets into equant, polygonal slabs ~5 m wide and 0.25 m thick. On steeper slopes, exposed polygonal slabs have domed surfaces; eroded slabs reveal an onion-like internal structure formed by 5-m-wide, second-order sheeting joints that terminate against the cross-joints, and may themselves be broken into polygons. In many structureless sandstone bodies, however, the lateral extent of first-order sheeting joints is severely limited by pre-existing, vertical tectonic joints. In this scenario, non-conjoined sheeting joints form extensive agglomerations of laterally contiguous, polygonal domes 3–6 m wide, exposing exhumed sheeting joints. These laterally confined sheeting joints are, in turn, segmented by short vertical cross-joints into numerous small (~0.5 m) polygonal rock masses. We hypothesize that the sheeting joints in the Navajo Sandstone form via contemporaneous, land-surface-parallel compressive stresses, and that vertical cross-joints that delineate polygonal masses (both large and small) form during compression-driven buckling of thin, convex-up rock slabs. Abrasion of friable sandstone during runoff events widens vertical tectonic joints into gullies, enhancing land-surface convexity. Polygonal rock slabs described here provide a potential model for interpretation of similar-appearing patterns developed on the surface of Mars.

INTRODUCTION

Sheeting joints are opening-mode fractures that typically have convex-up curvature and form at shallow depth (<100 m) with no discernible offset (Martel, 2017). Long viewed as "unloading structures" requiring removal of thick overburden, sheeting joints (like "A-tents" and "pop-ups"; Jahns, 1943; Romani and Twidale, 1999; Twidale and Bourne, 2003) have more recently been interpreted as products of compressive stresses parallel to exposed rock surfaces (Holzhausen, 1989; Bahat et al., 1999; Martel, 2011, 2017). These stresses can be perturbed by local topography, so landscapes have strong influences on the distribution and abundance of fresh, fractured rock (Miller and Dunne, 1996; St. Clair et al., 2015; Slim et al., 2015). At shallow depth, compressive stress parallel to convex land surfaces induces tension perpendicular to the surface, allowing sheeting joints to open (Martel, 2011, 2017).

Sheeting joints are prominent and well known from outcrops of homogenous granite, but they are also well developed in some stratified sandstones (Bradley, 1963; Bahat et al., 1995). Formation of these joints is not restricted to active plate boundaries; contemporaneous stresses are also forming them on cratons and passive margins (Twidale and Bourne, 2009). Polygonal fracture patterns can develop in tabular granitic masses generated by sheet jointing (Riley et al., 2012); such patterns are also prominent in sheet-jointed Navajo Sandstone (west-central Colorado Plateau, USA). The sheeting joints we describe possess most of the fundamental characteristics of sheeting joints in granite, but the interactions of surface-parallel stresses, buckling, and gullying have generated spectacular, small-scale landforms that are unknown from granite or any other rock type. The purpose of this field-based study is to describe and interpret the structures, patterns, and landforms developed in sheet-jointed outcrops of the Jurassic Navajo Sandstone of southern Utah (Fig. 1).

While the lateral scale and low curvature of some sheeting joints in the cross-stratified Navajo Sandstone are reminiscent of those seen in other areas (e.g., Sierra Nevada granite, western USA; Gilbert, 1904; Matthes, 1930; Martel, 2011), we show here that, in southern Utah, sheet-jointed sandstone can form expansive composite landforms that resemble pans of giant bread muffins. Clusters of polygonal domes extend for hundreds of meters, but each exposed, convex sheeting joint measures <5 m in diameter (Fig. 2).

In our study areas, the shapes and scales of most individual sheeting joints are strongly constrained by the spacing, continuity, and orientation of vertical joints. We will refer to some of these vertical joints (which are unrelated to topographic stresses) as "tectonic joints" (appearing as bold black lines in our diagrams). Also present are vertical cross-joints that form polygonal pat-

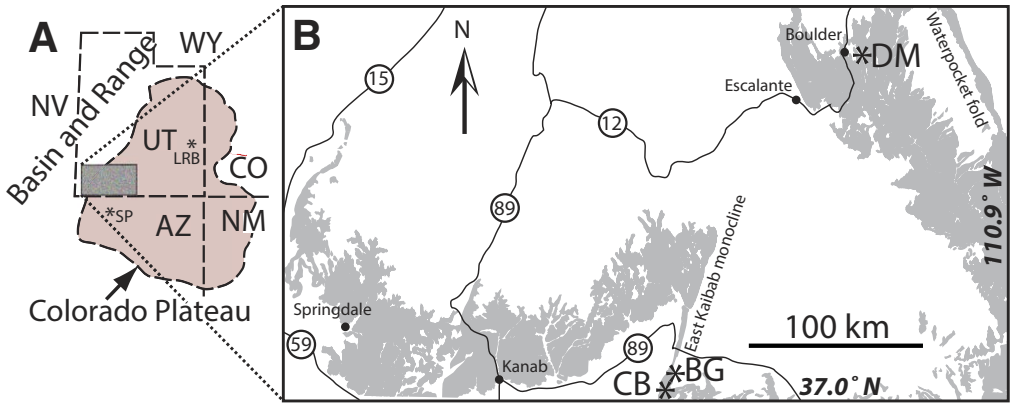

Figure 1. (A) Location of Colorado Plateau (red) and study area (gray). Two sites mentioned in Fig. 4 lie outside the study area: Little Rainbow Bridge (LRB) and Sowats Point (SP). WY—Wyoming; UT—Utah; CO—Colorado; AZ—Arizona; NM—New Mexico. (B) Outcrop map of Jurassic Navajo Sandstone (gray) showing locations of the three southern Utah study sites: Coyote Buttes (CB), Buckskin Gulch (BG), and Durfey Mesa (DM).

Figure 2. Landforms controlled by strongly convex sheeting joints at Buckskin Gulch, southern Utah (37.045°N, 111.995°W, WGS84). Each 3–6-m-wide domed surface is an exhumed sheeting joint. Narrow gullies cut by runoff accentuate the boundaries between the large polygons. The smaller polygons are laterally bounded by short, vertical joints that abut the over- and underlying sheeting joints.

terns (thin black lines). Because sheeting joints (red lines) are opening-mode fractures, they cannot propagate across the voids generated by other opening-mode fractures. Compressive stresses can, however, be transmitted, albeit in a perturbed state, across pre-existing vertical joints in the near surface (Rawnsley et al., 1992; Homberg et al., 1997; Zhao et al., 2008).

Compared to granite, most thick, wind-blown sandstones, although well sorted, are quite heterogeneous. The bulk of the Navajo Sandstone is composed of large-scale, eolian cross-strata; thin laminations were deposited across dune slopes by migrating wind ripples, and coarser, thicker, grain-flow strata record dry avalanches that moved down dune slip faces (Hunter, 1977). Here, we hypothesize that the presence or absence of small-scale inhomogeneities—namely stratification—dictate the development (or non-development) and geometry of sheeting joints in the Navajo Sandstone. Stratified Navajo Sandstone outcrops host large-scale planar sheeting joints, but such rocks rarely host smaller-scale, second-order sheeting joints. These smaller, strongly curved joints are, however, spectacularly developed in what we here refer to as structureless sandstone—isotropic rock in which primary (depositional) features have been destroyed. During the Jurassic, two processes obliterated primary sedimentary structures in parts of the Navajo Sandstone: bioturbation (Sanderson, 1974; Loope and Rowe, 2003) and liquefaction (Horowitz, 1982; Bryant and Miall, 2010). Bioturbation is widespread in many sedimentary facies, but relatively rare in the deposits of desert dunes. Most of the outcrops of structureless eolian sandstone exposed on the Colorado Plateau, including those discussed here, are best explained by liquefaction.

The genesis of young rock fractures is of obvious importance to the understanding of physical and chemical processes taking place in the critical zone where life flourishes (Anderson et al., 2007; Slim et al., 2015; St. Clair et al., 2015). Sheeting joints form parallel to sloping land surfaces, cut fresh rock, enhance infiltration of rainwater, and can control the flow direction of shallow groundwater (LeGrand, 1949; Martel, 2017). The distribution and active propagation of sheeting joints can also control the location, size, and timing of rockfall events (Stock et al., 2012; Collins and Stock, 2016). Runoff of surface water over the friable sandstone exposed in our study area rapidly cuts numerous small gullies that enhance local relief and land-surface convexity, thereby leading to development of steeply dipping sheeting joints. Sheeting joints break massive rock into material that can be transported. In the last 10 m.y., denudation of the Colorado Plateau has been dramatic. In this time interval, a thickness of ~1600 m of rock has been stripped from our study area (Lazear et al., 2013). The total volume of sediment carried by the Colorado River to the Gulf of California since 5.3 Ma is ~2.8×10^5 km^3 (Dorsey and Lazear, 2013).

In this paper, we consider the west-central region of the Colorado Plateau where the Navajo Sandstone is exposed and cut by two generations of sheeting joints. Here, we (1) show how tectonic joints control the distribution of first-order sheeting joints; (2) present a hypothesis for the origin of the polygonal, vertical cross-joints that abut underlying first- and second-order sheeting joints; and (3) briefly explore the interplay between meter-scale erosional and deformational processes.

PREVIOUS STUDIES

Stratified and Structureless Navajo Sandstone

The Navajo Sandstone, a Lower Jurassic quartz arenite, was deposited in a giant dune field near the western edge of Pangea (Kocurek and Dott, 1983). The preserved deposits of this erg extend from central Wyoming to southeastern California. The formation is ~400 m thick in south-central Utah, but it thickens westward, reaching 600 m in southwestern Utah (Blakey et al., 1988). Although large-scale cross-strata dominate nearly all Navajo outcrops, scattered lacustrine carbonate lenses in southern Utah and northern Arizona (Parrish et al., 2017) indicate that, during Navajo deposition, the regional water table lay at shallow depth below the dunes. In comparison to typical Navajo strata, the Navajo at our Coyote Buttes and Buckskin Gulch study areas (Fig. 1) contains thicker and more numerous grain-flow (avalanche) cross-strata (Loope et al., 2001). The rocks at these sites are also coarser and more friable than at other Navajo outcrops. Upon erosion, friable sandstones yield an abundance of easily transported, abrasive particles; this makes their outcrops vulnerable to both wind and water erosion (Loope et al., 2008, 2012).

Large masses of structureless sandstone are numerous in Navajo Sandstone outcrops exposed along the East Kaibab monocline in southern Utah and northern Arizona. The large percentage (by volume) of grain-flow strata in these outcrops helps to account for the abundance of structureless sandstone (Loope et al., 2012; Bryant et al., 2013): in shallow, water-saturated subsurface settings, unlithified grain flows are more easily liquefied by seismic shaking than the tighter-packed, wind-ripple deposits (Hunter, 1981). Although some of the structureless sandstone at Coyote Buttes is bioturbated (Loope and Rowe, 2003; Loope, 2006; Ekdale et al., 2007), contorted strata adjacent to and surrounding the structureless masses show that large volumes of originally stratified sand were homogenized during seismic shocks (Fig. 3; Bryant and Miall, 2010; Bryant et al., 2013). Isolated, angular blocks of stratified sandstone are common within the bodies of structureless sandstone that were homogenized presumably during paleo- seismic shocks (Fig. 3B).

Tectonic Joints in Sandstone

Bradley (1963) called attention to the near ubiquity of large-scale sheeting joints in the thick sandstones of the Colorado Plateau, described those joints as similar to those in crystalline rocks (especially in their parallelism to land surfaces), and argued that they play key roles in the origins of topographic domes and exfoliation "caves" or alcoves. He also noted that sheeting joints (in general) are scarce in heavily fractured rock, and that they are not controlled by rock textures or structures. In his study of rock mechanics of the Navajo Sandstone at Zion National Park in southwestern Utah, Robinson (1970) showed that cross-stratified Navajo Sandstone is strong in compression (70 MPa) and weak in tension (3.0–1.2 MPa parallel to bedding, 1.0–0.5 MPa perpendicular to

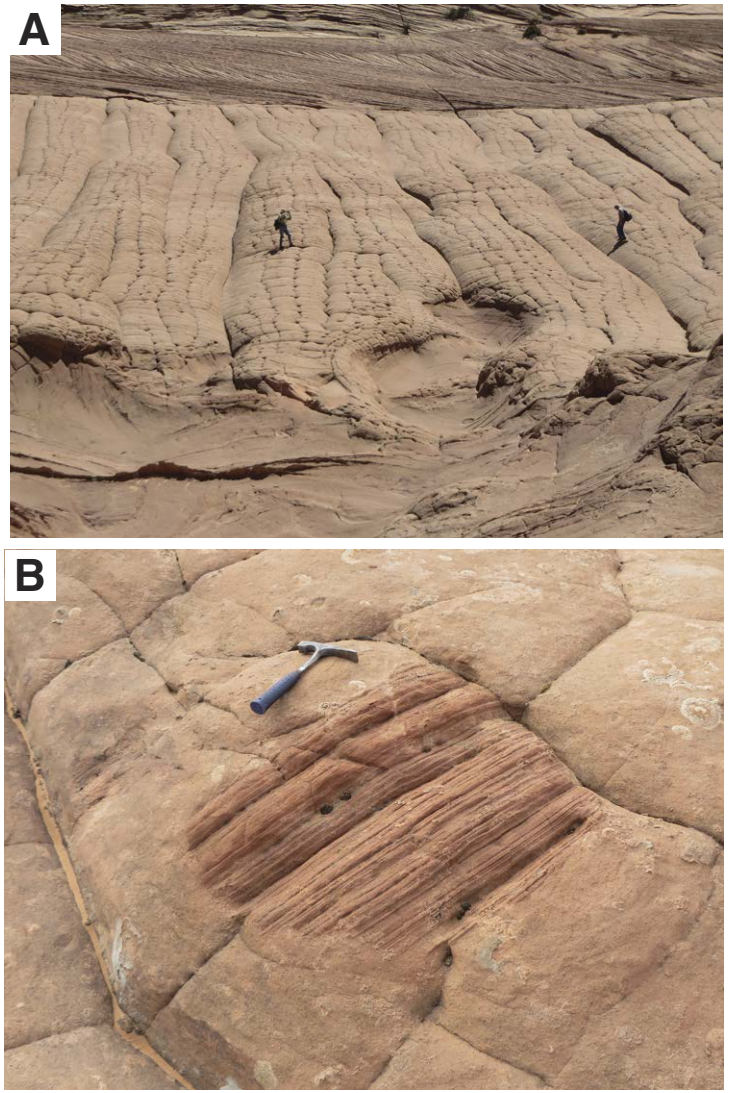

Figure 3. Relationships between structureless and stratified sandstone. (A) (37.04581°N, 111.9925°W) Lower one-third of the image comprises large-scale, cross-stratified sandstone that was deformed during soft-sediment deformation. Bulbous masses of deformed cross-strata contact jointed, structureless sandstone (middle part of image, with people for scale). Undeformed cross-strata (uppermost part of image) lie above the structureless sandstone. (B) (37.03630556°N, 111.996944°W) Isolated block of wind-ripple-laminated sand that was engulfed by liquefied sand (now represented by structureless sand with polygonal joints).

bedding). For comparison, granite is much stronger (130 MPa in compression and 4.8 MPa in tension) (Engineering ToolBox; https://www.engineeringtoolbox.com/compression-tension-strength-d_1352.html). Bahat et al. (1995) studied the morphologies of the features developed on the surfaces of sheeting joints in Zion National Park and used them to better understand joint initiation and propagation.

Hodgson (1961) mapped the trends of tectonic joints and observed sandstone fracture surfaces in southeastern Utah. Much of his data on joint orientation came from the Navajo Sandstone, but his observations and insights regarding plumose structure and other fracture-surface textures came from finer-grained Permian sandstones and siltstones. In their study of the East Kaibab monocline, Mollema and Aydin (1999) mapped a set of E- to ESE-trending tectonic joints at one of the sites included in our study (Buckskin Gulch; Fig. 1). They concluded that those fractures post-date Laramide folding, that they are the youngest tectonic structures in their mapped area, and that they probably coincide in age with regional joint sets attributed by Bergerat et al. (1992) to late-stage Laramide compression. This is consistent with the late stage of Laramide compression noted by Yonkee and Weil (2015).

Joint-Trace Patterns and Infilling Joints

Olson and Pollard (1989) showed that the pattern, shape, and extent of overlap of tectonic joint traces depends on the difference between the greatest and the least regional horizontal compressive stresses (S_H and S_h respectively). Branching joints with overlapping en echelon cracks that curve toward each other develop when local stresses dominate over remote stresses; in contrast, straight joints develop when the remote differential stress is crack parallel and compressive (Renshaw and Pollard, 1994).

After initial widely spaced joints form, tectonic infilling of gaps between those joints continues (Gross, 1993); the infilling joints may be parallel or perpendicular to the later-forming joints. In their study of the origins of orthogonal joint sets, Bai et al. (2002) showed that orthogonal patterns can develop without a 90° rotation of the regional stress field if the spacing of the joints relative to the bed thickness is less than a critical value of the ratio of the intermediate and maximum horizontal principal stresses.

Surface-Parallel Stresses and Sheeting Joints

Sheeting joints open parallel to the land surface, where crustal stress perpendicular to the land surface (σ_3) is zero, and σ_1 and σ_2 are parallel to the land surface (Fossen, 2010). Surface geometry has been shown to strongly influence stresses at shallow depth (Miller and Dunne, 1996). Miller and Dunne (1996) and Martel (2011) showed that, where vertical stress is strongly reduced and local topography has high curvature, local surface-parallel compressive stresses can be set up in, for example, the downslope and the contour-parallel

directions. Martel (2011, 2017) argued that remote, surface-parallel compressive stresses, together with gravity and topographic convexity, can generate sufficient tensile stress to account for the opening of sheeting joints in granite of the Sierra Nevada. He showed that topographic domes are especially likely to be underlain by sheeting joints because there, compressive stresses (σ_1 and σ_2) are additive. Leith et al. (2014a) considered spalling in underground excavations to be closely analogous to sheeting joints. They argued that both phenomena develop at sites of high differential stress created by exhumation because with unloading, the vertical crustal stress component (S_v) typically diminishes more rapidly than the S_H and S_h components (Leith et al., 2014a).

Surface-Parallel Stresses and A-Tents

Adams (1982), Romani and Twidale (1999), and Twidale and Bourne (2003, 2009) argued that A-tents are (like sheeting joints) neotectonic manifestations of surface-parallel compressive stress. A-tents combine two rock-fracture components: a sheeting joint (the base of the "A") and the high-angle fracture between the two tilted slabs (making the sides of the "A"). A-tents in Sierra Nevada granite have apertures as great as 0.6 m (Ericson and Olvmo, 2004), demonstrating the considerable stresses involved in their buckling. Surface-parallel compressive stresses between 10 and 30 MPa have been measured at sites where sheeting joints and A-tents in granite are present (Martel, 2006). On the Colorado Plateau, surface-parallel stresses are probably weaker, but the tensile strength of the Navajo Sandstone is much less than that of granite.

Although we have not found A-tents associated with sheeting joints at our study areas in south-central Utah, they are present, but rare, in the Navajo Sandstone of southeastern Utah and in the Permian Esplanade Sandstone of western Grand Canyon, Arizona (Fig. 4). The presence of these A-tents suggests that surface-parallel compressive stresses strong enough to buckle and break sandstone are present in at least some portions of the Colorado Plateau.

Polygonal Patterns

The polygonal patterns described here have attracted little attention from previous workers. Early work suggested that polygonal cracks in rock units might be a result of contraction of a "crust" or "rind" developed as a result of weathering (Williams and Robinson, 1989). Polygonal patterns in the Navajo Sandstone were named "elephant-skin weathering" by Howard and Selby (2009). Polygonal fractures are variously attributed to weathering, desiccation, thermal stresses, or diagenesis of clays (Johnston, 1927; Netoff, 1971; Howard and Selby, 2009; Riley et al., 2012; Goehring, 2013). Chan et al. (2008) interpreted the polygonal fracture patterns at Checkerboard Mesa, Utah, as products of tensile weathering stresses caused by temperature and moisture fluctuations and suggested that they may be good analogs for interpreting similar-appearing polygons in the Utopia Planitia region of Mars.

STUDY AREAS

We studied sheeting and vertical joints in the Navajo Sandstone at three main localities in south-central Utah (Buckskin Gulch, Coyote Buttes, and Durfey Mesa; Fig. 1). The features we describe are within the Colorado River drainage basin, at elevations (above sea level, asl) between 1975 m (Durfey Mesa) and 1510 m (Buckskin Gulch).

For Durfey Mesa, the nearest weather station (Boulder, Utah, 2050 m asl) recorded a mean annual temperature (1981–2010) of 10.00 °C; (mean January high = 4.00 °C, low = –6.33 °C; mean July high = 28.2 °C, low = 15.9 °C). Mean annual precipitation was 288.04 mm (mean August maximum = 43.69 mm). At the nearest weather station to Buckskin Gulch (Page, Arizona, 1307 m asl), the mean annual temperature was 15.08 °C (mean January high = 6.61 °C, low = –0.83 °C; mean July high = 33.06 °C, low = 21.11 °C). Mean precipitation was 211.08 mm (mean August maximum = 29.72 mm). Above weather data are from the National Centers for Environmental Information (https://www.ncdc.noaa.gov/cdo-web/datatools/normals).

EXTENSIVE SHEETING JOINTS: DESCRIPTION

The great majority of sheeting joints in our study areas are <5 m wide, but in at least two outcrops at Coyote Buttes, stacks of broad sheeting joints can be traced for hundreds of meters (Fig. 5). At one of these sites, these joints cut structureless sandstone (Fig. 5A), but at the other site (0.25 km away), they cut a single, thick set of eolian cross-strata (individual cross-strata can be traced directly across numerous sheeting joints; Fig. 5B). At the structureless outcrop, all sheeting joints closely follow rolling topography (Fig. 5A), but at the stratified outcrop, all 19 of the exposed sheeting joints are nearly horizontal despite the outcrop's steep slopes (Fig. 5B). Although vertical spacing of sheeting joints in granite typically increases with depth normal to the land surface (Holman, 1976; Martel, 2017), we have not observed this trend in our study areas: for example, the 19 near-horizontal sheeting joints shown in Figure 5B do not show such a trend.

In structureless sandstone (Fig. 6), short, vertical cross-joints that abut under- and overlying sheeting joints subdivide the broad rock slabs into a hexagonal pattern defined by triple junctions. The hexagonal pattern of cross-joints does not develop in well-stratified sandstone slabs. The hexagonal slabs in the structureless sandstone are equant and range in diameter (including measurements both parallel and normal to slope) from 215 to 595 cm, averaging 348 cm (n = 24, Buckskin Gulch; Table 1). The angle of many (but not all) fracture intersections approaches 120°; the patterns resemble those illustrated by Pollard and Aydin (1988, their figures 15G, 15H). On slopes greater than ~10°, the upper surfaces of hexagonal slabs are domed (Fig. 6B), but on near-horizontal land surfaces, these slabs have flat tops (Fig. 6A). The domed surfaces of the hexagonal slabs at Buckskin Gulch have smooth curvatures averaging 0.17° cm^{-1} (Table 1). These measurements correspond to the curvatures of spheres with

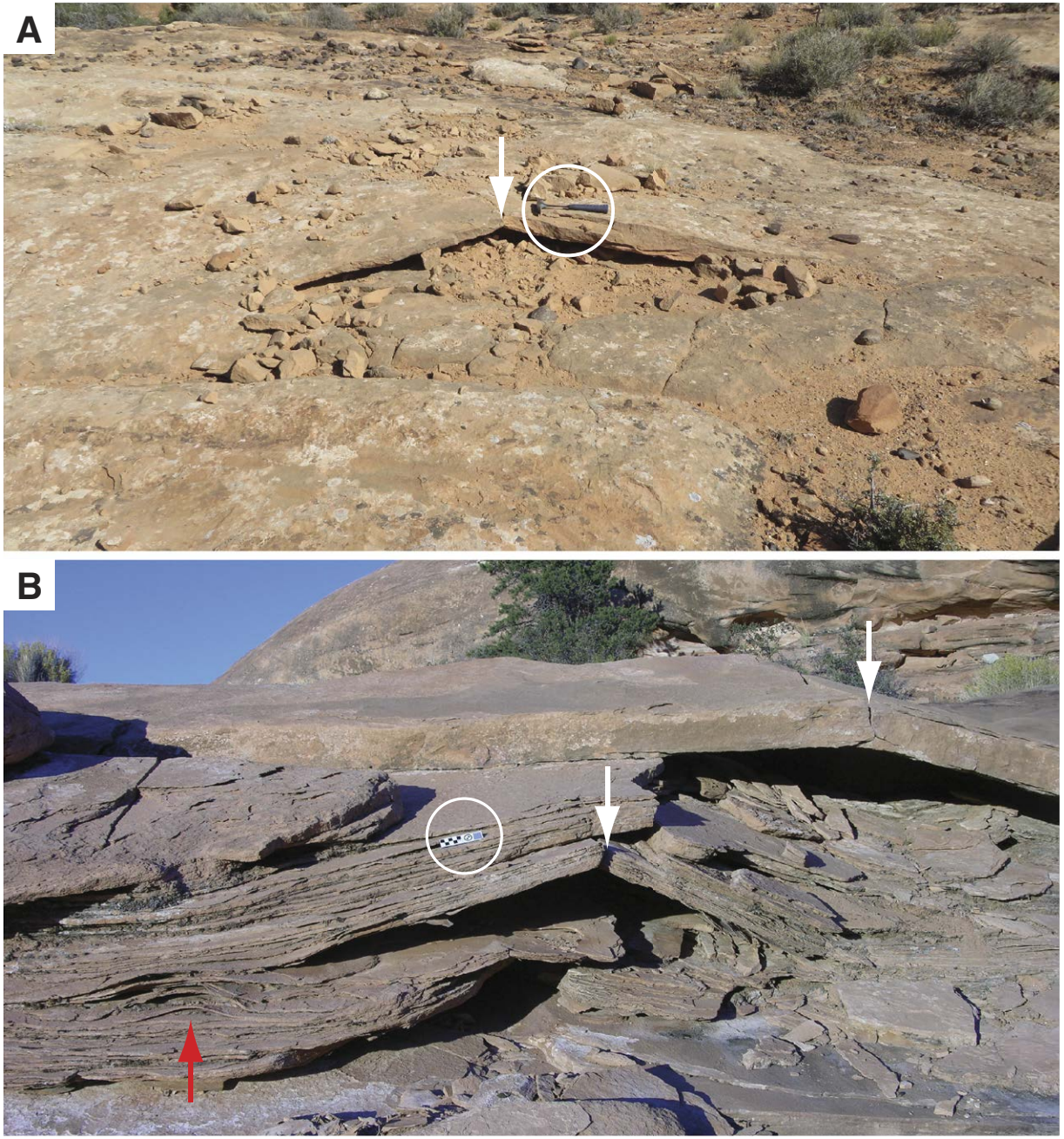

Figure 4. A-tents in Colorado Plateau sandstones outside the study area (Fig. 1). Arrows mark crests of structures. (A) A-tent in the Navajo Sandstone. Note freshly broken, angular pieces of sandstone surrounding the structure, and hammer (circled) for scale (southeastern Utah; trail to Little Rainbow Bridge; 38.5768°N, 109.6278°W, WGS 84; photo taken 3 June 2017). (B) (36.521432°N, 112.553692°W) A-tents (white arrows) and a blister (red arrow) in the Permian Esplanade Sandstone; scale bar (circled) is 15 cm long (below Sowats Point, Grand Canyon, Arizona).

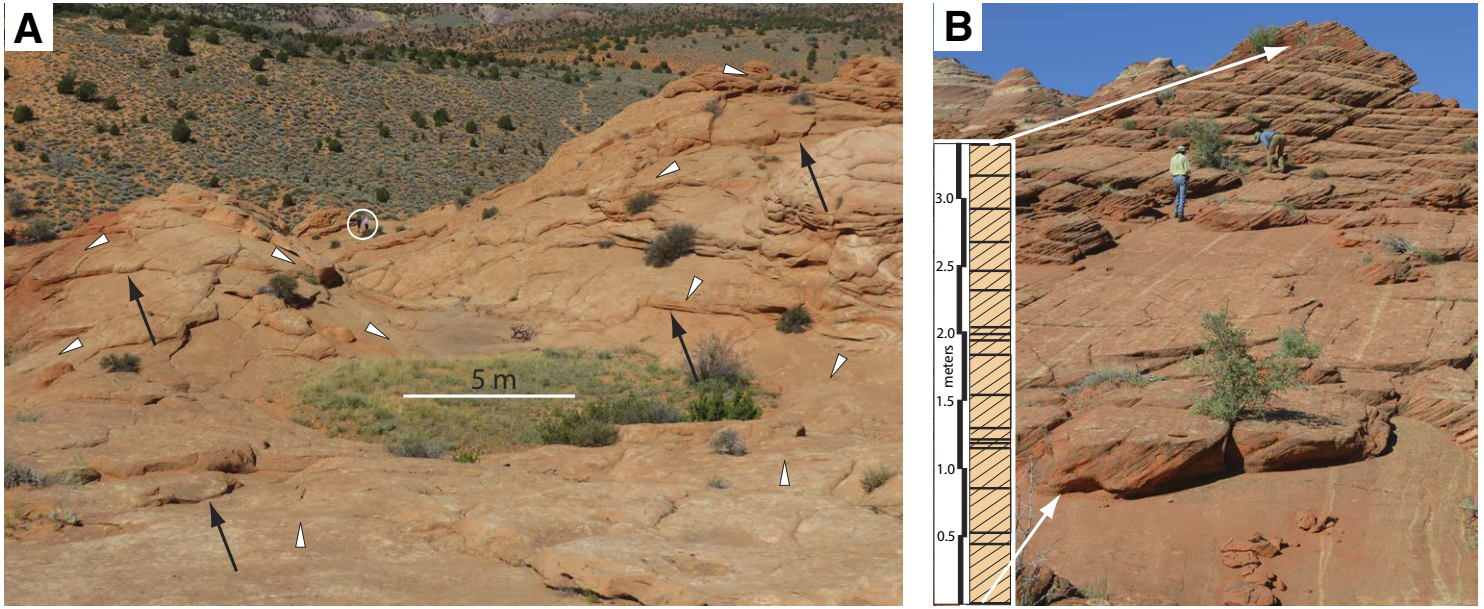

Figure 5. Laterally extensive sheeting joints at Coyote Buttes, southern Utah. (A) (37.013014°N, 112.007277°W) Undulating topography underlain by parallel, undulating sheeting joints. Each white triangle points in the direction of slope and rests on an exposed sheeting joint; each black arrow points to a sheeting joint that is under- and overlain by a tabular rock slab. Two geologists in the middle distance are circled. (B) (37.0126944°N, 112.00722°W) A single, thick set of eolian cross-strata (dipping left) is cut by at least 19 low-angle sheeting joints. Rock sheets bounded by these joints (arrows) range from 45 cm to 2.5 cm thick (mean 21 cm; standard deviation 12 cm). Geologist on left stands on a sheeting joint that can be traced for tens of meters. Photo by Bob Jackson.

radii averaging 349 cm. Erosion of the dome-topped slabs reveals their onion-like structure (Fig. 6B).

Domed sheeting joints at Coyote Buttes are lightly eroded, but not gullied (Fig. 6B). Compared to the average curvature and radius of curvature of the gullied domes at Buckskin Gulch (0.18° cm^{-1} and 360 cm), the average curvature of Coyote Buttes domes (0.10° cm^{-1}) is much less and the average radius of curvature (1074 cm) is nearly three times that of the Buckskin Gulch domes (Table 1).

The surfaces of the first-order (3–6-m-diameter) polygons are, in turn, broken into smaller (~0.5-m-diameter) second-order polygons (Figs. 6B, 6C). As with the large polygons, these smaller polygons are produced by planar, high-angle, non-tectonic joints that terminate against the sheeting joints (Figs. 6B, 6C).

EXTENSIVE SHEETING JOINTS: INTERPRETATION

In our study area, nearly all sheeting joints lie parallel to the land surface and are associated with abutting cross-joints (Figs. 5A, 7). In areas with steep topography, steeply dipping sheeting joints commonly occur at higher positions on outcrops than near-horizontal sheeting joints (Fig. 7). Like the lower sheeting joints shown in Figure 7, the near-horizontal sheeting joints shown in Figure 5B likely formed when their host rocks occupied a near-horizontal hilltop. We conclude that at the site where sheeting joints cut stratified sandstone (Fig. 5B), mass wasting and granular disintegration have outpaced sheet jointing—the near-horizontal sheeting joints are out of equilibrium with the steep slopes of their immediate surroundings.

We do not have an explanation for why the sheeting joints in our study area do not show the increase in spacing with depth (Fig. 5B) that is typically seen in granite terrains. We note, however, that the sandstone outcrops in our study area provided no opportunities to observe sheeting joints in vertical cross-sections >3.5 m.

Second-order sheeting joints terminate against the vertical cross-joints that abut the extensive first-order sheeting joints (Figs. 6B, 6C); these formed at shallower depth after erosion increased the convexity of the land surface. We hypothesize that the (older) first-order cross-joints as well as the (younger) vertical cross-joints that terminate against the second-order sheeting joints were produced by the same stresses that generated the sheeting joints—land-sur-

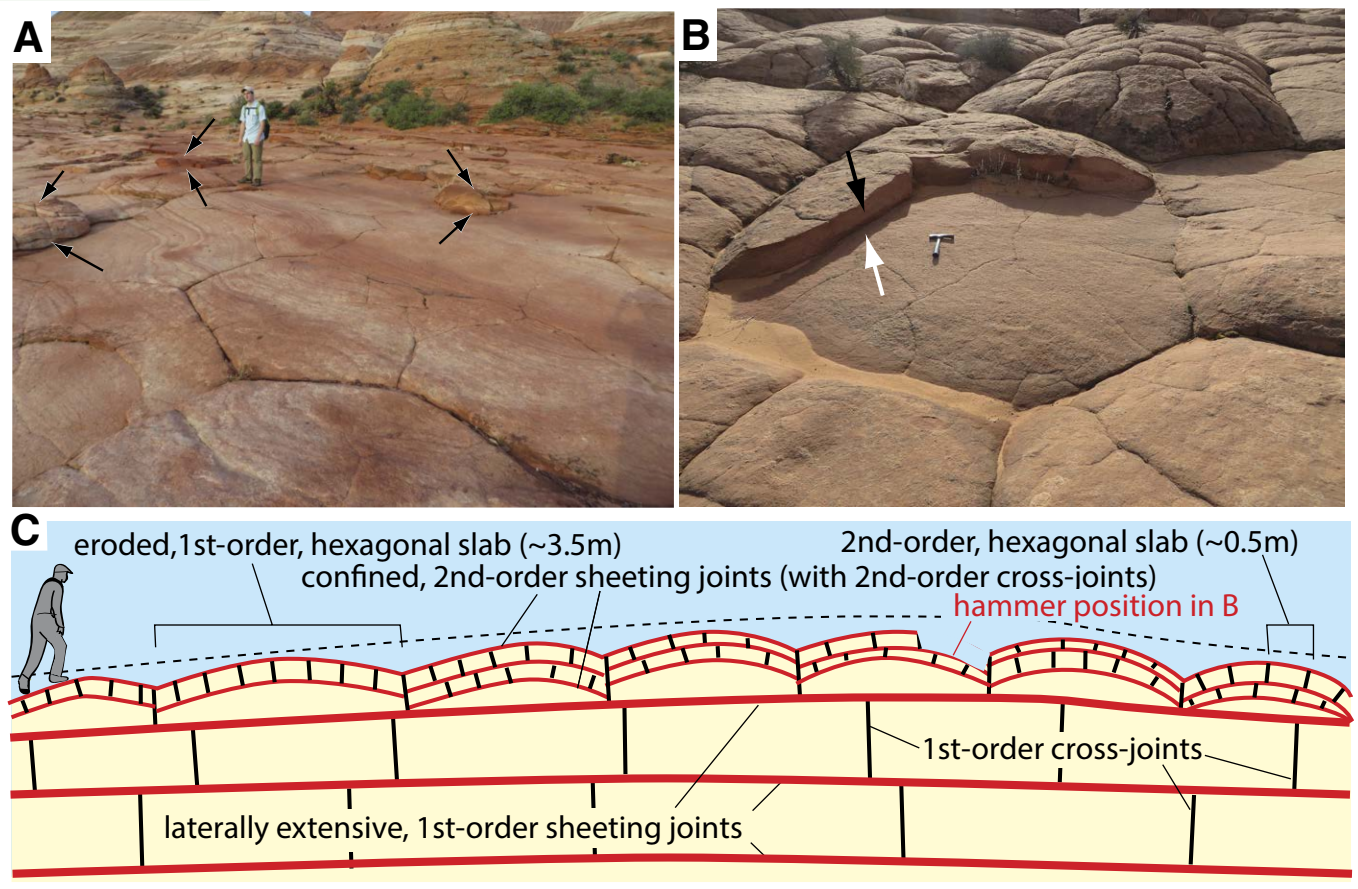

Figure 6. Sheeting joints and polygonal patterns. (A) Arrows mark surfaces of broad, nearly horizontal sheeting joints that extend for tens to hundreds of meters. Large, flat-topped (first-order) hexagonal slabs are bounded laterally by abutting, vertical, non-tectonic cross-joints (Coyote Buttes, southern Utah; 37.0082°N, 112.0078°W). (B) (37.044344°N, 111.994166°W) Conjoined, hexagonal domes in sheet-jointed sandstone. A convex, recently exposed, second-order sheeting joint (white arrow and hammer) lies below the weathered remnants of the surface of a higher sheeting joint (black arrow)—the elements of an "onion-like structure". Note the second-order polygonal patterns formed at the upper terminations of vertical cross-joints that abut the exposed, convex sheeting joints. (C) Interpretive diagram of a broad, domed topographic surface underlain by two generations of parallel sheeting joints (red lines). In the uppermost, eroded rock slab, second-order sheeting joints abut first-order cross-joints (long black lines) and terminate second-order, vertical cross-joints (short black lines). Erosion along the vertical joints of the uppermost rock sheet increased the convexity of the large hexagons. The resulting, enhanced convexity led to development of secondary convex sheeting joints and their abutting secondary cross-joints. Tectonic joints are absent. Dashed line shows approximate position of former (now eroded) sheeting joint.

face-parallel compression (Fig. 8; Martel, 2011, his figure 3; Leith et al., 2014a, their figure 2b; see Stresses, below). The small-scale polygons are analogs (fractals) of the large-scale polygons and formed by the same processes. Buckling (Figs. 6C, 8)—either during or immediately after propagation of the underlying sheeting joint—best explains (1) the uniformity and the broad extent of the patterns formed by the cross-joints and (2) the repetition with depth of the same patterns with the same scales in successive, separate slabs (Figs. 6, 7). In this model, the first-order rock slab created by the first-order sheeting joint is still subjected to lateral compression from all directions in which there is a curvature of the land surface. This lateral compression generates a bend in the rock slab and an outer-arc stretch, leading to the development of the subvertical fractures in the sheet (Lemiszki et al., 1994). Polygonal patterns can form if there is curvature (and therefore an outer-arc stretch) in all directions, plausible in a domed land surface. The individual first-order polygons are then broken into second-order slabs as second-order sheeting joints develop (Fig. 6). These second-order slabs may also be subject to buckling. The lower tensile strength, the lower fracture toughness, and the much greater curvature of the sandstone sheeting joints (Table 1) compared to those developed in granite of the Sierra Nevada (Collins and Stock, 2016; Holman, 1976; Martel, 2017; Mitchell, 2010)—assuming that the spacing of sheeting joints of the two rock types is the same—make the sandstone more likely to fracture during the outer-arc stretch that is generated during buckling.

We have previously noted that A-tents (Fig. 4) are rare in the Navajo Sandstone on the Colorado Plateau and are not found in our study area, but polygonal systems of cross-joints are well developed. The primary factor determining which of these two structures forms is the proximity of the newly

TABLE 1. DIAMETERS AND CURVATURES OF DOMED SLABS AT BUCKSKIN GULCH AND COYOTE BUTTES, SOUTHERN UTAH

#	L_x (cm)	L_y (cm)	Minimum L / maximum L	θ_{x1} (°)	θ_{x2} (°)	R_x (cm)	C_x (° cm^{-1})	θ_{y1} (°)	θ_{y2} (°)	R_y (cm)	C_y (° cm^{-1})
Buckskin Gulch											
1	478	470	0.98	70	15	322	0.18	19	19	709	0.08
2	310	405	0.77	69	12	219	0.26	39	19	400	0.14
3	504	595	0.85	63	19	352	0.16	55	25	426	0.13
4	429	415	0.97	52	2	455	0.13	51	35	277	0.21
5	215	330	0.65	38	19	216	0.27	32	33	291	0.20
6	428	474	0.9	83	17	245	0.23	54	48	266	0.22
7	297	463	0.64	30	10	425	0.13	56	41	274	0.21
8	543	465	0.86	58	8	471	0.12	52	40	290	0.20
9	400	543	0.74	42	8	458	0.12	39	33	432	0.13
10	404	580	0.7	44	16	386	0.15	44	34	426	0.13
11	400	342	0.86	49	2	449	0.13	39	53	213	0.27
12	360	446	0.81	55	7	333	0.17	41	40	316	0.18
Mean	397	461	0.81	33		361	0.17	39		360	0.18
Coyote Buttes											
13	335	320	0.96	48	3	376	0.15	11	14	733	0.08
14	415	525	0.79	38	8	517	0.11	12	15	1114	0.05
15	530	505	0.95	49	8	533	0.11	11	7	1608	0.04
16	405	440	0.92	48	7	422	0.14	22	8	840	0.07
Mean	421	448	0.91	26		462	0.13	13		1074	0.06
Grand mean	403	457	0.83	31		386	0.16	33		538	0.15

Note: Diameters (L) were measured in two perpendicular directions—one parallel to the slope of the outcrop (x), the other perpendicular to that slope (y); dip angles (θ) were measured at termini of both measured diameters (where the sheeting joints abut vertical cross-joints). θ_1 was measured at the downslope terminus; θ_2 at the upslope terminus. Radius of curvature $R = 57.3 \times L / (\theta_1 + \theta_2)$; curvature $C = 360 / (2\pi R)$.

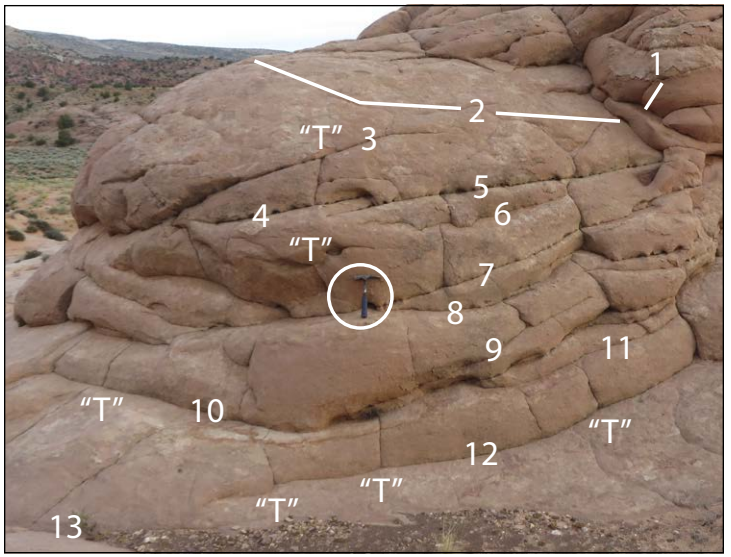

Figure 7. Thirteen planar to convex-up sheeting joints (numbered) exposed in a small, isolated sandstone butte. Hammer (circle) for scale. Each sheeting joint is abutted by vertical joints that terminate at "T" junctions. The sheeting joints at the base of the butte (10–13) lie parallel to the general land surface, but do not lie parallel to the proximal land surface. The sheeting joints higher on the butte (1–3) are parallel to the adjacent, steep sides of the butte (Buckskin Gulch, southern Utah; 37.047706°N, 111.992533°W.

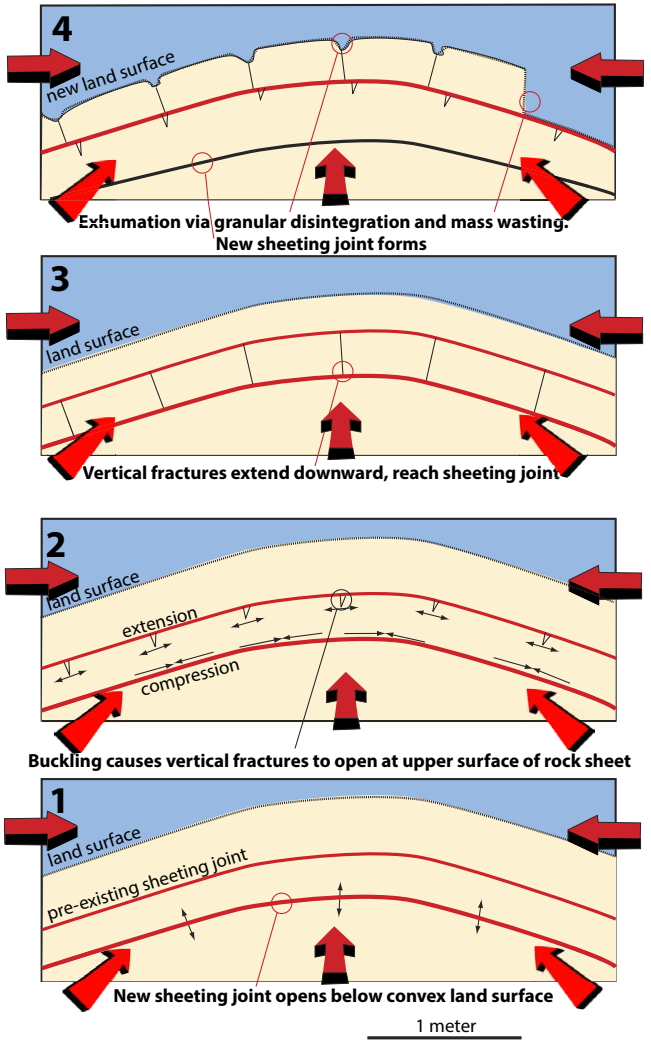

Figure 8. Sequence of events leading to the development of sheeting joints in the Navajo Sandstone. (1) Initiation of a new, subsurface sheeting joint due to contemporary land-surface-parallel compression of a topographic dome (cf. Martel, 2011, his figure 3). Radially inward-directed, compressive stresses (red arrows) cause buckling of the newly formed slab. (2) Buckling, in turn, causes extensional cracks to form at its upper surface (a pre-existing sheeting joint). (3) Cracks propagate downward, terminating at the new sheeting joint. (4) As the Colorado Plateau is exhumed, a new sheeting joint and associated vertical cross-joints form in the subsurface, the sheeting joint formed in stage 1 has reached the surface, and rock slabs bounded by cross-joints that formed in stages 2 and 3 slide down the land surface. Runoff and weathering widen the tops of the exposed cross-joints. No tectonic joints are shown.

formed sheet to the surface—sheets exposed to a free surface are more prone to developing A-tents than sheets forming in the subsurface, as greater buckling can be accommodated at the free surface. Following the work of Buck (1997) who showed that a thin plane under a certain compressive stress will "snap" whereas a thick plate under the same compressive stress will buckle and display minor outer-arc stretching, we speculate that the thickness of the rock sheet above the newly formed sheeting joint is also a factor in the type of secondary feature that develops. Where the rock sheet is relatively thin, snapping occurs, and an A-tent forms. Where the rock sheet is thicker, the sheet buckles, and outer-arc extension forms the polygonal joints. The amount of buckling required to either snap or crack the sheet may be quite small—Olson et al. (2009) showed that relatively small tensile stresses are required to break sandstone masses.

Although we favor surface-parallel, compression-induced buckling as the process that leads to formation of the polygonal fracture patterns in our study area, stresses due to diurnal thermal cycling also need to be considered as the dominant process (Riley et al., 2012) or at least as a supporting process (Eppes et al., 2016) in their generation (see Discussion).

LATERALLY CONFINED SHEETING JOINTS: DESCRIPTION

Over a large portion of our study areas, tectonic joints prevent sheeting joints from propagating more than 5 m. Hundreds of sheeting joints at Buckskin Gulch terminate against a single set of closely spaced, vertical tectonic joints (Fig. 9); the sheeting joints are therefore elongate and narrow, with surface areas up to 250 m^2 (Figs. 10–12). At Durfey Mesa, sheeting joints terminate against two sets of closely spaced, orthogonal joints and are thus equant and small (<25 m^2) (Fig. 13).

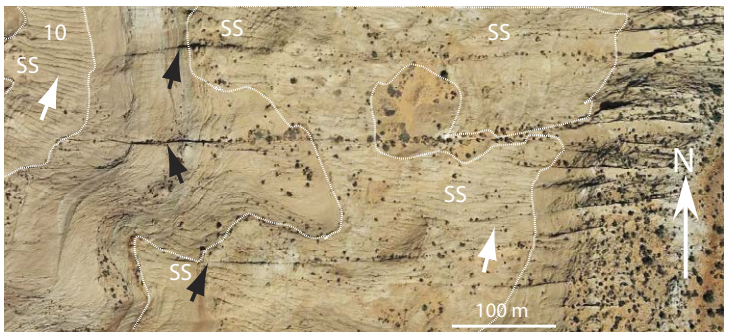

Figure 9. Google Earth image (Buckskin Gulch, southern Utah; center of image is 37.044°N, 111.988°W) showing widely spaced, straight east-west joints (black arrows) and infilling, curving joints that are closely spaced (white arrows). The closely spaced joints curve to become tangential to the widely spaced joints (lower black arrow). Parallel, convex-up sheeting joints discussed in this paper (Fig. 10) connect many of the closely spaced joints. White line shows the extent of structureless sandstone (SS); "10" is the location of rocks shown in Figure 10A.

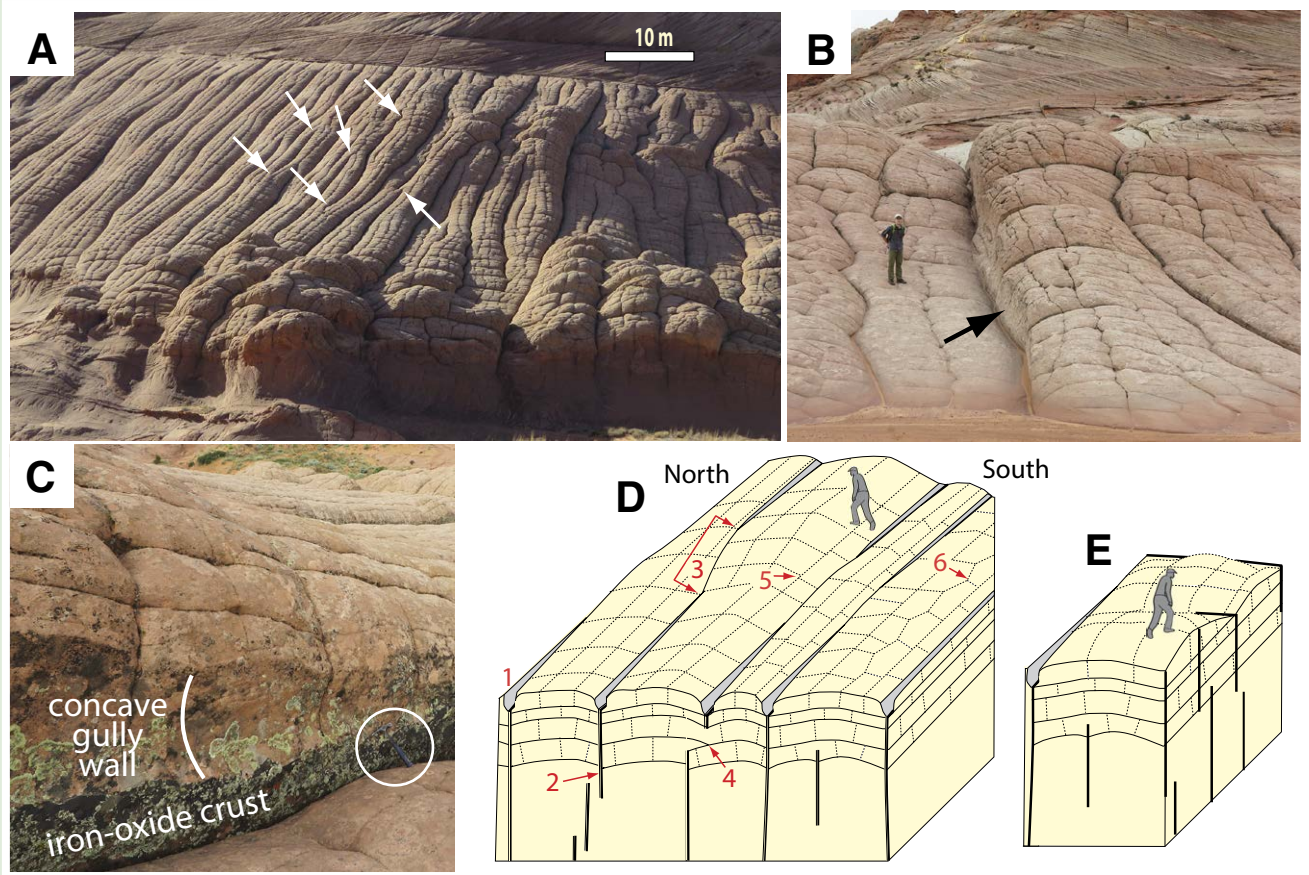

Figure 10. Control of sheeting joints and runoff by a set of vertical tectonic joints at Buckskin Gulch, southern Utah. The upper surface of each ridge is an exposed sheeting joint; tectonic joints are marked with white arrows in A. (A) (37.046°N, 111.9916°W) Oblique view of loaf-like landforms developed on structureless sandstone cut by parallel, closely spaced tectonic joints. Note the sharp boundary between unjointed, cross-stratified rocks (uppermost part of image) and jointed, structureless rocks. (B) (37.04619722°N, 111.99138889°W) Joint-bounded parallel ridges; arrow points to the gullied joint shown in C. Location is several hundred meters north (to the left) of A. (C) (37.0465833°N, 111.991388°W) Downslope view of the southern, concave wall of an exhumed gully. Crusts composed of iron-oxide-cemented sandstone are present along the left (southern) margins of the vertical, tectonic (east-west) joints. Joints act as gutters for runoff. Southern walls with iron-oxide cements are more resistant to erosion, and commonly stand in strong relief. Rock hammer (circled) for scale. (D) Vertical, tectonic joints (1) control locations of gullies. When seen in two-dimensional vertical section, most sheeting joints terminate against vertical joints (2). Like other opening-mode joints, sheeting joints cannot propagate across a void. The three-dimensional shapes of exhumed sheeting joints suggest that while in the shallow subsurface, some sheeting joints bridged laterally adjacent, but discontinuous, vertical joints. As gullying increased relief, new sheeting joints dipped more steeply—parallel to the steep, gullied walls. The in-plan geometries of some sheeting joint terminations suggest that sheeting joints can "jump" the lateral span between adjacent en echelon tectonic joints (3). Sheeting joints terminate not only against vertical tectonic joints, but also against adjacent sheeting joints (4). Short, vertical cross-joints terminate against the sheeting joints; contour-parallel cross-joints terminate against earlier-formed, slope-parallel cross-joints. In some areas, the ladder-like, orthogonal pattern (5) is absent, and polygons dominate (6). (E) Orthogonal network of vertical, tectonic joints controls the shape of sheeting joints; best developed at the Durfey Mesa study site.

Buckskin Gulch

At Buckskin Gulch (Fig. 1), east-west–oriented, tectonic, vertical joints cut the Navajo Sandstone. These joints are divisible into two subparallel sets (Fig. 9). Straight, widely spaced joints are laterally continuous for several hundreds of meters, and cut across both stratified and structureless rocks. Fractures within a second set of closely spaced anastomosing joints (Fig. 10) extend for <100 m and are most prominent in structureless sandstone. Some of these joints abut the straight, widely spaced joints at angles of <20°, but most bend to become tangential to the older, straighter joints (Fig. 9). In areas where the younger, anastomosing, tectonic joints are oriented subparallel to the slope direction of outcrops (Fig. 10), sheeting joints and loaf-like landforms are abundant. The sheeting joints are exposed as convex-up and slope-elongated land surfaces that are oriented parallel to the trend of the tectonic joints (Figs. 10, 11). Abrasion during runoff events down these slopes has led to downcutting and widening along the joints, forming gullies (Fig. 10). Southern walls of these east-west gullies are steeper than northern walls and stand in relief above them. Iron-oxide cement is abundant in the sandstone adjacent to the southern margins of the tectonic joints (Fig. 10B).

Elongate sheeting joints terminate against the closely spaced tectonic, vertical joints (feature 2 in Fig. 10D). With a tape, we measured the widths of eight of the sheeting joints perpendicular to a 12° slope; sheeting joints widths range from 2.35 m to 5.65 m (mean = 4.18 m; standard deviation = 1.25 m). In plan view, along the slope direction, the widths of individual sheeting joints vary; some taper over a short distance and terminate. Due to the lim-

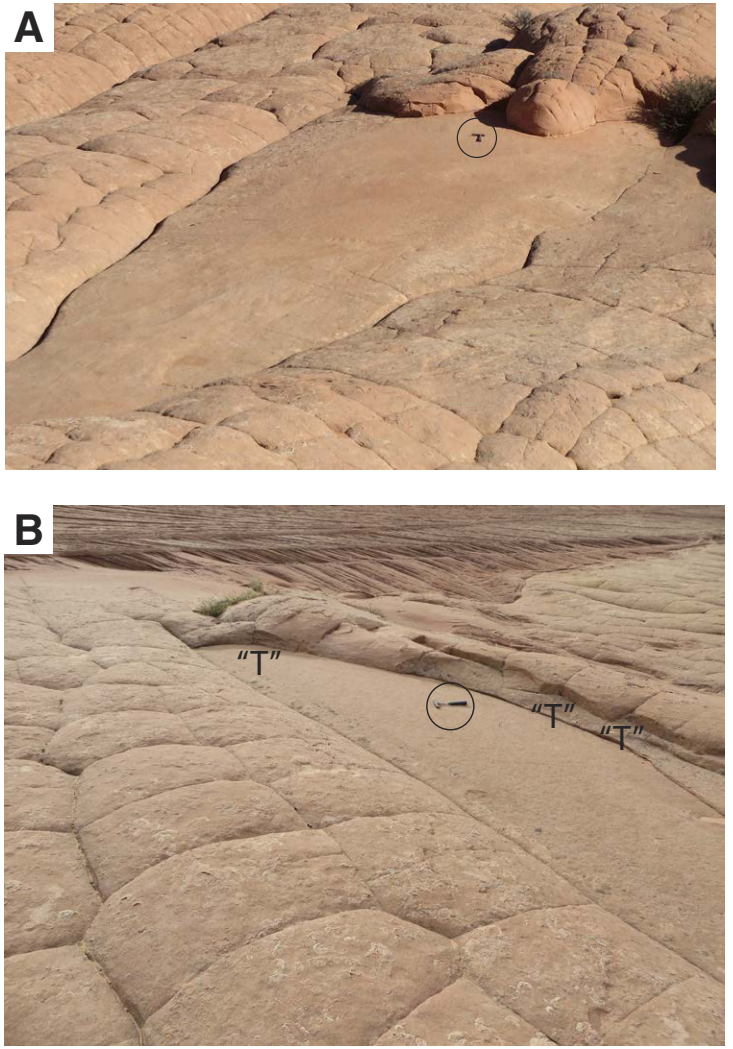

Figure 11. Recently exposed, slope-elongated, convex-up sheeting joints (under hammers) that abut the parallel, closely spaced joint set exposed at Buckskin Gulch, southern Utah (37.047144°N, 111.990556°W). Slope of loaf-like rock surfaces is 12°–14°. (A) The jointed and weathered rock slab upslope from the hammer is the remains of an elongate slab that once covered the smooth surface that extends downslope from the hammer. The smooth surface is also jointed in a pattern like the higher slab and surrounding slabs, but weathering has not opened the joints. (B) (37.04619722°N, 111.0413889°W) Pattern on the weathered sheeting joint in the left foreground shows a polygonal to orthogonal distribution of short, vertical cross-joints that abut the now-weathered sheeting joint and an underlying sheeting joint. In middle part of the photo, "T"s mark points where vertical joints meet an underlying sheeting joint that dips to the lower right.

Figure 12. Ladder-like pattern of joints at Buckskin Gulch, southern Utah (37.04619722°N, 111.99138889°W). Five slope-parallel tectonic joints (black lines at photo margins) control the overall geometry in this image; each of the six ridges is capped by a weathered sheeting joint. On a smaller scale, each convex-up sheeting joint is met by scores of short, vertical cross-joints. Slope-perpendicular cross-joints abut slope-parallel cross-joints, producing "T" junctions. Some cross-joints in this setting, however, meet at 120° angles (see Figs. 10, 11).

ited extent of outcropping structureless sandstone, erosion, and overlap by overlying rock sheets, we were unable to measure the maximum extent of these sheeting joints parallel to slope, but some are at least 60 m long. We measured the dips of exposed sheeting joints at their two (slope-perpendicular) lateral terminations with a Brunton compass, and calculated radii of curvature using the compass method (Carlson et al., 2005; in which $R = 57.3 \times L / D_c$, where R is radius of curvature in centimeters, L is length of the curve in centimeters, and D_c is the sum of the two dips in degrees). The radii of curvature of these eight sheeting joints range from 441 cm (curvature 0.13° cm^{-1}) to 164 cm (0.35° cm^{-1}); a circle with a radius of 57 cm has a curvature of 1.0° cm^{-1}.

Short, vertical cross-joints segment all of the rock slabs bounded by the convex-up sheeting joints. At Buckskin Gulch, the relationships between the cross-joints and the tectonic joints are well exposed (Fig. 12). Along the parallel tectonic joints, the short, vertical cross-joints, oriented both parallel and perpendicular to slope, segment the elongate, convex-up rock sheets into parallelepipeds that, in plan, form an extensive, ladder-like, orthogonal pattern (Fig. 12). Locally, the ladder-like pattern changes to a polygonal pattern (Fig. 11B).

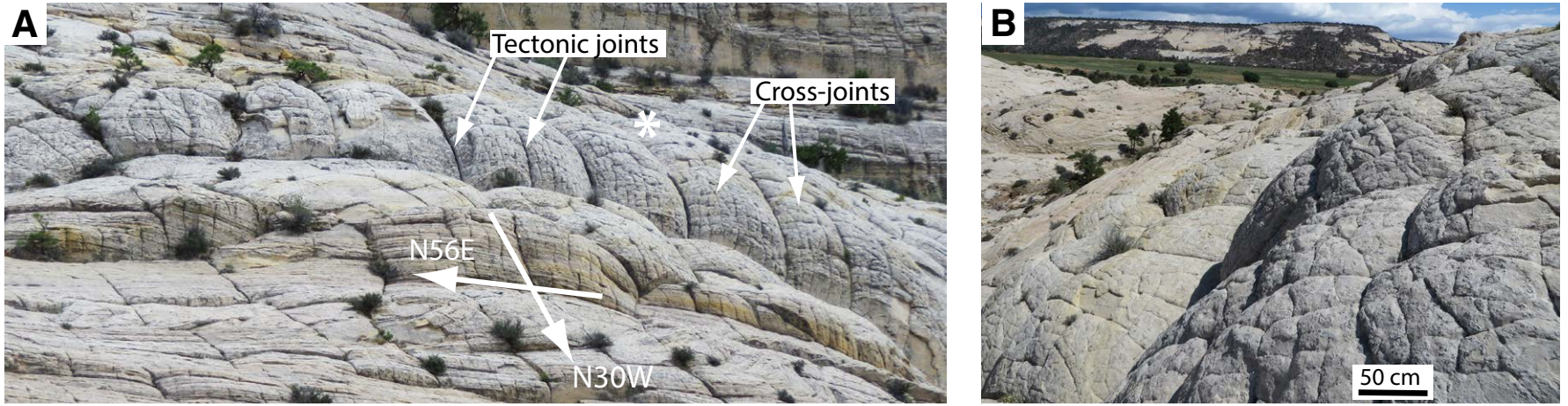

Figure 13. (A) Strongly convex, exposed sheeting joints (to left of and below asterisk) that are controlled by a large-scale (5 m) orthogonal pattern of tectonic joints at Durfey Mesa (37.8872°N, 111.4024°W). (B) View from the asterisk in A, looking back toward camera position for A. Note that the cross-joints visible on each of the exposed sheeting joints also form an orthogonal pattern.

Durfey Mesa

In and near the town of Boulder, Utah, sheeting joints are well exposed along the slopes of Durfey Mesa. Equant, 3–5-m-scale polygonal patterns at Durfey Mesa, like all the other domed polygonal landforms in our study areas, are controlled by pre-existing vertical joints. The joints that define the perimeters of domed polygons at Durfey Mesa, however, are tectonic (compare Figs. 6C and 10E). Tectonic joints at many sites in this area have an orthogonal pattern (Fig. 13). The dominant set of vertical tectonic joints is oriented ~N50°E, and a second, subordinate set is oriented ~N30°W. The sheeting joints that develop between the orthogonal joints are equant and limited to <5 m in diameter. On the steep slopes of the mesa, the joints (where polygons meet) are commonly gullied (Fig. 14A).

LATERALLY CONFINED SHEETING JOINTS: INTERPRETATION

At Buckskin Gulch, the shapes and lateral extents of sheeting joints are controlled by the position of closely spaced, subparallel, overlapping vertical joints of tectonic origin (Fig. 10). Because the closely spaced tectonic joints terminate against the straight, widely spaced joints or curve to become tangential to them, they are the younger of the two tectonic joint sets. Lateral terminations of vertical, en echelon tectonic joints are not easily seen in aerial imagery (Fig. 9), but the patterns that are developed on the exposed surfaces of the sheeting joints that terminate at those joints (feature 3 in Fig. 10D) indicate their subsurface positions.

Following Olson and Pollard (1989), we interpret the younger, closely spaced set of tectonic joints as infilling joints that propagated in a stress field in which local stresses were dominant over remote stresses. The anastomosing joints preferentially infilled the structureless (homogeneous) rocks between the early, straight joints that cross-cut both structureless and stratified rocks.

As with the extensive sheeting joints at Coyote Buttes, we interpret the elongated sheeting joints at Buckskin Gulch (Figs. 10, 11, 12) as products of compressive, land-surface-parallel stresses that generated tensile stress perpendicular to the land surface (Martel, 2011; Leith et al., 2014a; Bahat et al., 1999). The pre-existing tectonic joints greatly limited the slope-perpendicular extent of the sheeting joints. Because most of the slope-perpendicular cross-joints abut the slope-parallel cross-joints in the ladder-like patterns at Buckskin Gulch (Figs. 10, 11, 12), they (generally) formed later. The local change of the ladder pattern into a polygonal pattern of the same scale, however, suggests that all of the cross-joints along the entire length of the elongate sheeting joints formed during a single episode of outer-arc stretching. The long axes of ladders at Buckskin Gulch developed parallel to the tectonic joints (Figs. 10–12) and perpendicular to the direction of strongest curvature of the hosting sheeting joints. The joints composing the ladder axes thus trend perpendicular to the direction of greatest surface-parallel stress ($\sigma_{11}k_1$ of Martel, 2011). These relationships support buckling of a convex, elongate rock slab above an opening, convex, elongate sheeting joint as the best explanation for the origin of the tensile stresses that formed the cross-joints (Fig. 8; see Discussion).

As noted by Martel (2011), erosion generates convexity—a precondition for most sheeting joints. Initially, rainwater runoff down a freshly exposed sandstone with downslope-parallel joints would have been concentrated along the

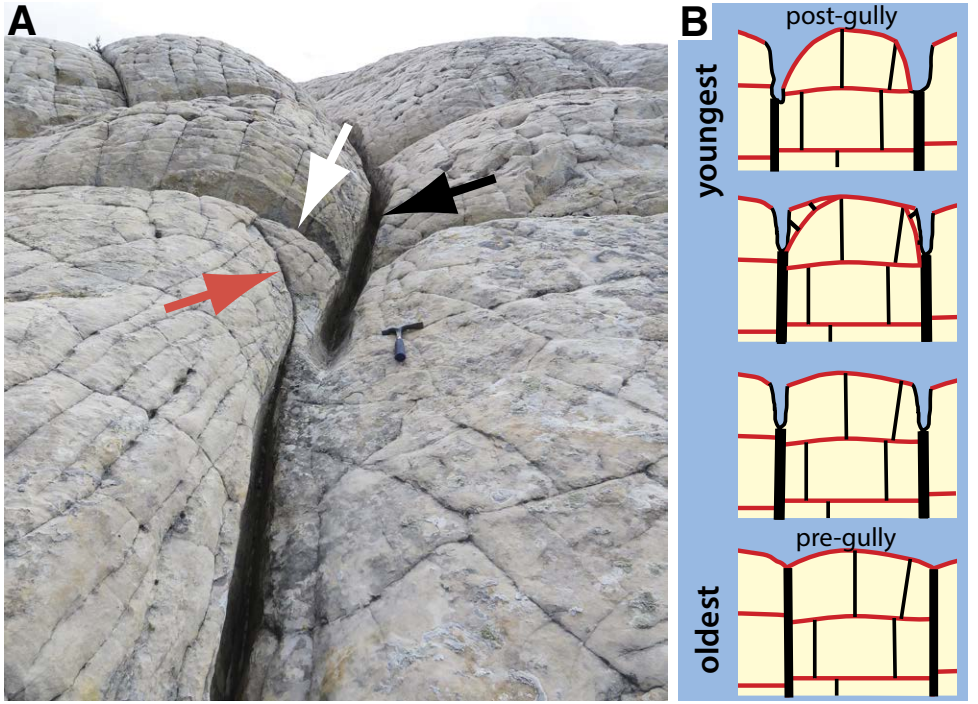

Figure 14. Interaction of erosion and jointing. (A) Structures exposed between convex sandstone surfaces on the slope of Durfey Mesa, southern Utah (37.04619722°N, 111.0413889°W): a gully incised by sand-laden runoff (black arrow); an adjacent (exhumed) convex sheeting joint (white arrow); a steeply dipping sheeting joint (red arrow); and two vertical, overlapping tectonic joints. Our interpretation is that the upper part of the gully occupies the lower, proximal termination of one vertical tectonic joint; the less-steep sheeting joint joins the upper tectonic joint, and the steeply dipping sheeting joint terminates at the distal end of a second, deeper, overlapping tectonic joint. The steeply dipping sheeting joint is likely the youngest joint shown. (B) Interactions of sheeting joints and topography. Tectonic joints are bold, black, vertical lines; cross-joints are thin black lines; sheeting joints are red lines. (1) Low-relief land surface is underlain by horizontal sheeting joints. (2) Gullies cut by runoff along vertical tectonic joints increase relief. (3) New sheeting joints with steep dips form subparallel to gullies (analogous to red-arrowed joint in A); the lateral extents of new sheeting joints are limited by the distribution of the vertical, cross-joints. (4) The new land surface reaches equilibrium with gullying and jointing; younger sheeting joints have steeper dips.

joints. Convex "pioneer" sheeting joints were likely to develop beneath each of the narrow, elongated land surfaces bounded by the parallel tectonic joints. With continued exhumation, new generations of convex sheeting joints developed beneath them, thereby perpetuating water-shedding, convex ridges that prevented lateral coalescence of rivulets on the hillslope.

The southern (but not the northern) walls of the tectonic joints are cemented by iron oxide (Figs. 10B, 10C). The iron-oxide cements are the oxidized remnants of siderite cements that (because of degassing of CO_2-rich fluids) preferentially formed in sandstone on the downflow sides of joints (Loope et al., 2010). These iron-rich cements make the sandstone that composes the southern walls more resistant to erosion, so sheeting joints with high curvature cap the southern walls (Fig. 10B).

At Durfey Mesa, domed sheeting joints (Figs. 10E, 13, 14) were controlled by a pre-existing orthogonal pattern of tectonic joints. Orthogonal patterns of tectonic joints are commonly found in brittle sedimentary rocks. The dominant joints, oriented NE-SW at Durfey Mesa, and the subordinate NW-SE–oriented joints may have developed under the same stress field, or they may record a rotation of the tectonic stress field (Bai et al., 2002), but without knowledge of the ratio of the extant (or ancient) horizontal remote principal stresses, we cannot make this distinction. Our interpretation of the stress field that generated the sheeting joints in our study area (below) is independent of the stress field that generated the tectonic joints.

Laterally confined, convex sheeting joints are apparent only in structureless sandstone—its isotropic fabric (free of inhomogeneities that develop stress concentrations) makes it the strongest rock type in our study area. Martel (2006, 2017) noted that sheeting joints are conspicuously absent from weak rocks like shale because under large differential stress, they fail via shearing. Shang et al. (2016) showed that rocks with even incipient (poorly developed) bedding planes have tensile strengths only 32%–88% of those of a structureless "parent rock" without visible discontinuities (also see Zahm and Hennings, 2009). Because the structureless sandstone bodies had greater strength in compression than the bedded rock that surrounds them, they withstood high compressive stress and failed under tensile stresses when they neared the land surface. The isotropic fabric of the structureless sandstone also allowed opening-mode fractures to propagate along smooth curves. In the bedded sandstone, stress concentrations along abrupt changes in grain size increased internal shear stresses that led to sliding or tearing (mode 2 or mode 3 fractures; Leith et al., 2014b).

A typical sheeting joint in the Sierra Nevada (Martel, 2011) is convex, has an opening depth of 20 m, and has a land-surface-parallel radius of curvature (R)

of 1000 m. Using Martel's (2011) formulae, this curvature would be represented by k, where $k = –0.001$ m^{-1} and $R = 1/k$. By convention, convex curvature and compressive stress are given a negative sign (Martel, 2011). In the Utah study area, most sheeting joints have radii of curvature <10 m (Table 1; Fig. 6B) and much higher curvature ($k = 0.1$ m^{-1}). Opening depths can reach up to several meters (Fig. 5B), but most probably formed <1 m below the surface (Fig. 6B). As curvatures increase, the compressive stress required to open fractures diminishes (Martel, 2017, his figure 8). We estimate the stresses needed to open sheeting joints in the Navajo Sandstone beneath domed (axisymmetric) land surfaces using equation 5 from Martel (2011), that is:

$$\varphi = \sigma_{11}k_1 + \sigma_{22}k_2 - \rho g \cos ß, \quad (1)$$

where σ_{11} is the surface-parallel stress in one direction and σ_{22} is the surface-parallel stress in the perpendicular orientation, and g is the gravitational constant. The terms k_1 and k_2 respectively are the curvatures in those directions; we use +0.2 for each (both are positive due to the double convexity; Fig. 6B). We use the bulk density (ρ) of the Navajo Sandstone as 2300 kg m^{-3} (Robinson, 1970). Because k_1 and k_2 are both negative (due to double convexity) and σ_{11} and σ_{22} are both negative (due to compression), the products are both positive. If the land surface is horizontal, that is, the slope (β) is zero then the last term in the above equation is equal to 2.2563×10^4 Pa m^{-1}. Therefore, the combined stress-curvature terms must be greater than this relatively small value for φ to be positive—the necessary condition for a sheeting joint to nucleate.

At Olmstead Point in Yosemite National Park, California, Martel (2011) was able to estimate compressive and tensile stresses in his field area because previous overcoring measurements had yielded the orientation of σ_1 (120°) and the ranges of compressive stress for σ_1 and σ_2 (14–21 and 6.5–11 MPa respectively). These data had been obtained forty years earlier during a study carried out only 15 km from Olmstead Point (Cadman, 1970). Although data on near-surface horizontal stresses are unavailable for our study area and for our study region, we argue that due to the strong convex curvatures (k factors ~100 times those typical of the Sierra Nevada) and shallow depth of the Utah sheeting joints (<3.5 m), relatively low compressive stresses (two orders of magnitude less than those at Yosemite?) were likely required to open these joints. The probable low compressive surface-parallel stresses required are therefore plausible, given the modification of local stresses by topography, despite the fact that the Colorado Plateau is in an overall far-field extensional regime (Zoback and Zoback, 1980, 1989; Wong and Humphrey, 1989; Heidbach et al. 2009).

DISCUSSION

Convexity and Polygons

A large majority of the sheeting joints in our study area are convex up and occupy convex landscape elements—ridge tops, domes, and the slopes that surround domes (Figs. 2, 3, 6, 13, 14). Martel's (2011, 2017) model for the origin of sheeting joints, which emphasizes the importance of convex land surfaces in generating tensile stress for opening-mode fractures, fits the morphology and topographic context of sheeting joints in our field areas better than the exhumation hypothesis (Leith et al., 2014a), which was developed to explain sheeting joints on the floors and lower walls of glacial valleys. We attribute the three-dimensional hexagonal pattern of cross-joints that formed above each smooth, domed (axisymmetric) sheeting joint to compressive stresses that were directed radially inward (Fig. 8; Martel, 2011, his figure 3). As the outer rim of the strongly convex-up, equidimensional slab was subject to outer-arc stretching in all compass directions at once (the isotropic tension of Tuckwell et al. [2003]), cracking was initiated and a hexagonal fracture pattern rapidly developed above each new sheeting joint. A ladder-like orthogonal (rather than the hexagonal) pattern formed above convex sheeting joints that had greater curvature along one axis (Figs. 10–12). In these patterns, the longer (ladder-parallel) elements developed parallel to the axis of curvature of the elongate sheeting joints where the greatest tensile stresses were concentrated (analogous to A-tents; Fig. 4). The smoothly curved sheeting joints and the polygonal fracture patterns of the cross-joints do not fit as well with the strongly unequal lateral stresses suggested for the origin of sheeting joints by Leith et al. (2014a, 2014b; see also Martel, 2017).

Effects of Thermal Cycling on Sheet-Jointed Rock with Polygonal Patterns

Riley et al. (2012) attributed the polygonal joint pattern within sheet-jointed granite slabs of Yosemite National Park, California, to stresses generated at the land surface during diurnal thermal cycling. At their study area, the greatest average diurnal temperature fluctuations (27.8 °C) occur in August. According to their calculations (Riley et al., 2012, their figure 12), diurnal thermal stresses in granite outcrops diminish very rapidly with depth below the land surface. At the time of the minimum surface temperature (when tensile stresses are greatest), stress is 10.5 MPa at the surface and negligible at a depth of 283 mm (the depth where temperature fluctuations become negligible). This stress is sufficient to fracture granite (Riley et al., 2012). Their study, however, was limited to polygons on exposed slabs—the authors did not gather data on the subsurface depth to which polygon-bearing slabs extend. Photos showing cross-sections of sheeting joints and their abutting cross-joints in Yosemite (Martel, 2017, his figure 1i; Wolf, 2010) suggest that the process that generates the cross-joints in sheet-jointed granite continues to operate at least several meters below the land surface—far below the reach of diurnal thermal cycling.

At Coyote Buttes and Buckskin Gulch, June is the month with the greatest difference between average daily high and low atmospheric temperatures (14.72 °C; Page, Arizona; data from National Centers for Environmental Information, https://www.ncdc.noaa.gov/cdo-web/datatools/normals). This temperature range is only 49% of that in Yosemite. The thermal conductivity of

structureless quartz arenite, however, is about twice that of granodiorite. Using sandstone thermal diffusivity data from Hartlieb et al. (2016; K = 1.7 mm^2 s^{-1}), Shabbir et al. (2000; K = 1.5434 mm^2 s^{-1}), and Hanley et al. (1978; K = 1.8 mm^2 s^{-1}) and the formulae of Riley et al. (2012), the respective depths to T_0 (negligible temperature fluctuation) are 614 mm, 585 mm, and 632 mm respectively. Although tensile stresses due to thermal cycling are greatest at the land surface (Riley et al., 2012, their figure 12), vertical cross-joints that abut overlying sheeting joints form in the subsurface. Because polygonal networks are separated by opening-mode fractures, polygonal networks of cross-joints develop independently in each rock sheet. This requires that tensional stresses (in both California and Utah) had to be sufficient to initiate fracturing at multiple subsurface levels, not just at the land surface. The distribution of cross-joints at Buckskin Gulch (Fig. 7) suggests that some polygonal joint patterns at Buckskin Gulch (like those in Yosemite) formed at least 2.5 m below the land surface, well below the expected range of diurnal thermal cycling.

Experiments have shown that thermal stresses due to diurnal forcing can drive subcritical crack growth in granite boulders exposed to solar insolation. These stresses make rock more susceptible to cracking, especially when tension in the rock is enhanced for other reasons (Eppes et al., 2016). Fractures in boulders exposed to direct solar heating develop in specific orientations due to the diurnal change in the angle of insolation (Eppes et al., 2016, and references therein). On strongly curved rock surfaces in our study area (Fig. 2), the same polygonal patterns are developed on the north-facing and south-facing slopes, suggesting that stresses generated by differential insolation did not cause the fracturing.

Eppes et al. (2016) did not find that frost cracking—the slow growth of ice crystals within pre-existing fractures (Anderson, 1998)—was important to cracking of granite in their experiments, but the process could be more important in porous and permeable sandstones. Granular disintegration and joint widening take place at the land surface, but long-exposed sheeting joints in our study areas show the same jointing patterns and spacing that we see developed on newly exposed sheeting joints and in subsurface rock slabs visible in cross-section. Thermal processes play a role in the propagation and widening of sheeting joints (Stock et al., 2012; Collins and Stock, 2016). They also may be important in development of the polygonal joint networks that abut sheeting joints. Data on the subsurface vertical extent of the polygonal patterns developed in both sandstone and granite are needed to better understand the origin of the polygonal patterns in sheet-jointed rocks.

Landforms

Our observation that steeply dipping sheeting joints in the Navajo Sandstone commonly occur above near-horizontal sheeting joints (Fig. 7) is consistent with landform evolution: when near-horizontal land surfaces underlain by near-horizontal sheeting joints are dissected, steeply dipping sheeting joints are likely to form parallel to the steep slopes (Martel, 2011).

Erosion of the Navajo Sandstone forms narrow gullies (Fig. 14) during runoff events and thereby increases the relief of jointed rock surfaces (Figs. 10C, 10D). This erosion helps to explain the variation in curvature seen in Table 1. The key to generating high-relief polygons in the Navajo Sandstone is the channeling of runoff along their margins (Figs. 2, 14). The measured curvatures of polygons that have not been gullied (Fig. 6) are no more than half of those that show evidence of gullying (Fig. 2; Table 1).

Growth of steeply dipping sheeting joints requires steep land surfaces, and the steep land surfaces in our study area have resulted from the overland flow of water. Landscapes developed on structureless sandstone evolve as gullies incise the domed polygons. Because the lateral growth of subsurface sheeting joints along gullies is constrained by the distribution of near-vertical cross-joints (stage 3 in Fig. 14B), in early erosional stages only the sheeting joints directly adjacent to the gullies develop steep dips.

Implications for Planetary Geology

Polygonal crack patterns (as distinct from other patterned ground) are widespread on the northern plains of Mars, and are particularly difficult to explain in regions such as Utopia Planitia. The cracks have been attributed to a variety of mechanisms, including freeze-thaw weathering (e.g., Seibert and Kargel, 2001), desiccation (e.g., El Maarry et al., 2012), and thermal contraction (e.g., Levy et al., 2010). However, the Utopia Planitia features are much larger than those formed by these mechanisms on Earth (McGill, 1986; Hiesinger and Head, 2000). Chan et al. (2008) suggested that the polygons in the Navajo Sandstone (which they interpreted as weathering features) were in fact the most appropriate analogs for the Utopia Planitia structures. We suggest that although thermal processes may have aided the propagation of pre-existing fractures (Anderson, 1998; Martel, 2017), the polygonal patterns in the Navajo Sandstone are primarily the result of sheeting-joint development. Here, we briefly explore the implications of this idea for the polygonal terrain in Utopia Planitia.

Our model for polygonal fracture development is based on three key points: (1) following the model of Martel (2011), the land surface must have topography and curvature; (2) surface-parallel compressive stresses must exist; and (3) a tensile, surface-perpendicular stress can be set up that is greater than the final term in Martel (2011)'s equation 5, that is, $\rho g \cos ß$. Concerning point 1, McGill and Hills (1992) and Seibert and Kargel (2001) discussed the probability of buried topography under the most recent material in the Utopia Planitia, although they ascribe the formation of the polygons to differential compaction of this youngest layer over the topography. With respect to point 2, Searls and Phillips (2007) used finite element modeling to demonstrate that global tectonic compression is necessary to create the radial and concentric faults observed around Utopia Planitia. Similar results were obtained by Gudkova et al. (2017). Lastly, concerning point 3, for the Utopia Planitia region, the average material density is ~2700 kg m^{-3} (Searls and Phillips, 2007), the gravitational acceleration on Mars is 3.711 m s^{-2}, and the land surface has a slope of 0.1°

(Seibert and Kargel, 2001). We have no constraints on the curvature, but the sum of the curvature and stress in two mutually perpendicular directions must be >1.0020 × 10^4 Pa m^{-1}. Searls and Phillips (2007) show that the compressive stresses in the Utopia Planitia region must be on the order of 22–25 MPa. Our model is therefore plausible for the Utopia Planitia region, and future studies of Martian polygons should now consider the possibility that the Utopia Planitia polygons are products of surface-parallel compression.

CONCLUSIONS

1. Vertical joints constrain the lateral extent of sheeting joints in the Navajo Sandstone of the Colorado Plateau. Where tectonic joints are widely spaced or absent, near-horizontal to broadly undulating sheeting joints can extend for tens of meters. Where outcrops of structureless Navajo are cut by one or two sets of closely spaced (3–5 m) tectonic joints, sheeting joints are small and equant or narrow and elongated. With erosion, these fractures form large fleets of contiguous, muffin-like or loaf-like rock masses.

2. We interpret the laterally confined, convex sheeting joints in the Navajo Sandstone as products of tensile stress generated by surface-parallel compression (Martel, 2011, 2017); thermal stresses may have played a secondary role. The strong curvature of the land surfaces above these joints greatly reduced the compressive stress needed to form them.

3. In our study areas, shallow sheeting joints are always present beneath outcrops of structureless sandstone that are broken by polygonal joint patterns. The polygons are delineated by non-tectonic vertical cross-joints that abut underlying sheeting joints. We hypothesize that cross-joints form during buckling of convex-up rock slabs that accompanies formation of underlying sheeting joints. Formation of the polygonal pattern is analogous to formation of A-tents, except that A-tents form during two-dimensional, not three-dimensional, buckling.

4. Domed, polygonal landforms in southern Utah owe their strong convexity to the friability of their host sandstone and to the interplay between erosional incision and the surface-parallel compressive stresses that we presume generate sheeting joints.

5. Strong, isotropic rock is a prerequisite for development of strongly curved sheeting joints in the Navajo Sandstone. Seismic events in a Jurassic dune field with a high water table generated the structureless sand that now, as non-stratified sandstone, hosts a large percentage of the sheeting joints in our study areas.

6. Some polygonal fractures on the surface of Mars may be products of surface-parallel compressive stresses, as we hypothesize here for the Navajo Sandstone.

ACKNOWLEDGMENTS

This study was supported by funds from the Schultz Chair in Stratigraphy at the University of Nebraska. Cindy Loope, Anthony Kohtz, and Bob Jackson helped with field work. We appreciate the helpful feedback from Steve Martel, and the advice of Mindi Searls, David Pitts, and Kevin Loope. Thoughtful comments and suggestions by Atilla Aydin, Raymond Russo, and an anonymous reviewer allowed major improvements to this manuscript.

REFERENCES CITED

Adams, J., 1982, Stress-relief buckles in the McFarland quarry, Ottawa: Canadian Journal of Earth Sciences, v. 19, p. 1883–1887, https://doi.org/10.1139/e82-167.

Anderson, R.S., 1998, Near-surface thermal profiles in alpine bedrock: Implications for the frost weathering of rock: Arctic and Alpine Research, v. 30, p. 362–372, https://doi.org/10.2307/1552008.

Anderson, S.P., von Blanckenburg, F., and White, A.F., 2007, Physical and chemical controls on the Critical Zone: Elements, v. 3, p. 315–319, https://doi.org/10.2113/gselements.3.5.315.

Bahat, D., Grossenbacher, K., and Karasaki, K., 1995, Investigation of exfoliation joints in Navajo Sandstone at the Zion National Park and in granite at the Yosemite National Park by tectonofractographic techniques: Berkeley, California, Lawrence Berkeley Laboratory, 67 p.

Bahat, D., Grossenbacher, K., and Karasaki, K., 1999, Mechanisms of exfoliation joint formation in granitic rock, Yosemite National Park: Journal of Structural Geology, v. 21, p. 85–96, https://doi.org/10.1016/S0191-8141(98)00069-8.

Bai, T., Maerten, L., Gross, M.R., and Aydin, A., 2002, Orthogonal cross-joints: Do they imply a regional stress rotation?: Journal of Structural Geology, v. 24, p. 77–88, https://doi.org/10.1016/S0191-8141(01)00050-5.

Bergerat, F., Bouroz-Weil, C., and Angelier, J., 1992, Palaeostresses inferred from macrofractures, Colorado Plateau, western U.S.A.: Tectonophysics, v. 206, p. 219–243, https://doi.org/10.1016/0040-1951(92)90378-J.

Blakey, R.C., Peterson, F., and Kocurek, G., 1988, Synthesis of late Paleozoic and Mesozoic eolian deposits of the Western Interior of the United States: Sedimentary Geology, v. 56, p. 3–125, https://doi.org/10.1016/0037-0738(88)90050-4.

Bradley, W.C., 1963, Large-scale exfoliation in massive sandstones of the Colorado Plateau: Geological Society of America Bulletin, v, 74, p. 519–528, https://doi.org/10.1130/0016-7606(1963)74[519:LEIMSO]2.0.CO;2.

Bryant, G., and Miall, A., 2010, Diverse products of near-surface sediment mobilization in an ancient eolianite: Outcrop features of the early Jurassic Navajo Sandstone: Basin Research, v. 22, p. 578–590, https://doi.org/10.1111/j.1365-2117.2010.00483.x.

Bryant, G., Monegato, G., and Miall, A., 2013, Example of liquefaction-induced interdune sedimentation from the Jurassic Navajo Sandstone, USA: Sedimentary Geology, v. 297, p. 50–62, https://doi.org/10.1016/j.sedgeo.2013.09.001.

Buck, W.R., 1997, Bending thin lithosphere causes localized "snapping" and not distributed "crunching": Implications for abyssal hill formation: Geophysical Research Letters, v. 24, p. 2531–2534, https://doi.org/10.1029/97GL02640.

Cadman, J., 1970, The Origin of Exfoliation Joints in Granitic Rocks [Ph.D. dissertation]: Department of Civil Engineering, University of California-Berkeley, 117 p.

Carlson, P.J., Burris, M., Black, K., and Rose, E.R., 2005, Comparison of radius-estimating techniques for horizontal curves: Transportation Research Record: Journal of the Transportation Research Board (National Academies, Washington, D.C.), v. 1918, p. 76–83, https://doi.org/10.3141/1918-10.

Chan, M.A., Yonkee, W.A., Netoff, D.I., Seiler, W.M., and Ford, R.L., 2008, Polygonal cracks in bedrock on Earth and Mars: Implications for weathering: Icarus, v. 194, p. 65–71, https://doi.org/10.1016/j.icarus.2007.09.026.

Collins, B.D., and Stock, G.F., 2016, Rockfall triggering by cyclic thermal stressing of exfoliation fractures: Nature Geoscience, v. 9, p. 395–400, https://doi.org/10.1038/ngeo2686.

Dorsey, R.J., and Lazear, G.D., 2013, A post–6 Ma sediment budget for the Colorado River: Geosphere, v. 9, p. 781–791, https://doi.org/10.1130/GES00784.1.

Ekdale, A.A., Bromley, R.G., and Loope, D.B., 2007, Ichnofacies of an ancient erg: A climatically influenced trace fossil association in the Jurassic Navajo Sandstone, southern Utah, USA, *in* Miller, W., III, ed., Trace Fossils: Concepts, Problems, Prospects: Amsterdam, Elsevier, p. 562–574, https://doi.org/10.1016/B978-044452949-7/50161-3.

El Maarry, M.R., Kodikara, J., Wijessoriya, S., Markiewicz, W.J., and Thomas, N., 2012, Desiccation mechanism for formation of giant polygons on Earth and intermediate-sized polygons on Mars: Results from a pre-fracture model: Earth and Planetary Science Letters, v. 323–324, p. 19–26, https://doi.org/10.1016/j.epsl.2012.01.016.

Eppes, M.C., Magi, B., Hallet, B., Delmelle, E., Mackenzie-Helnwein, P., Warren, K., and Swami, S., 2016, Deciphering the role of solar-induced thermal stresses in rock weathering: Geological Society of America Bulletin, v. 128, p. 1315–1338, https://doi.org/10.1130/B31422.1.

Ericson, K., and Olvmo, M., 2004, A-tents in the central Sierra Nevada, California: A geomorphological indicator of tectonic stress: Physical Geography, v. 25, p. 291–312, https://doi.org/10.2747/0272-3646.25.4.291.
Fossen, H., 2010, Structural Geology: Cambridge University Press, 463 p.
Gilbert, G.K., 1904, Dome and dome structures of the High Sierra: Geological Society of America Bulletin, v. 15, p. 29–36, https://doi.org/10.1130/GSAB-15-29.
Goehring, L., 2013, Evolving fracture patterns: Columnar joints, mud cracks and polygonal terrain: Philosophical Transactions of the Royal Society of London, Series A: Mathematical and Physical Sciences, v. 371, 20120353, https://doi.org/10.1098/rsta.2012.0353.
Gross, M.R., 1993, The origin and spacing of cross-joints: Examples from the Monterey Formation, Santa Barbara Coastline, California: Journal of Structural Geology, v. 15, p. 737–751, https://doi.org/10.1016/0191-8141(93)90059-J.
Gudkova, T.V., Batov, A.V., and Zharkov, V.N., 2017, Model estimates of non-hydrostatic stresses in the Martian crust and mantle: 1—Two-level model: Solar System Research, v. 51, p. 457–478, https://doi.org/10.1134/S003809461706003X.
Hanley, E.J., Dewitt, D.P., and Roy, R.F., 1978, The thermal diffusivity of eight well-characterized rocks for the temperature range 300–1000 K: Engineering Geology, v. 12, p. 31–47, https://doi.org/10.1016/0013-7952(78)90003-0.
Hartlieb, P., Toifl, M., Kuchar, F., Meisels, R., and Antretter, T., 2016, Thermo-physical properties of selected hard rocks and their relation to microwave-assisted comminution: Minerals Engineering, v. 91, p. 34–41, https://doi.org/10.1016/j.mineng.2015.11.008.
Heidbach, O., Tingay, M., Barth, A., Reinecker, J., Kurfeß, D., and Müller, B., 2009, The World Stress Map based on the database release 2008: Paris, Commission for the Geological Map of the World, equatorial scale 1:46,000,000, https://doi.org/10.1594/GFZ.WSM.Map2009.
Hiesinger, H., and Head, J.W., 2000, Characteristics and origin of polygonal terrain in southern Utopia Planitia, Mars: Results from Mars Orbiter Laser Altimeter and Mars Orbiter Camera data: Journal of Geophysical Research, v. 105, p. 11,999–12,022, https://doi.org/10.1029/1999JE001193.
Hodgson, R.A., 1961, Classification of structures on joint surfaces: American Journal of Science, v. 259, p. 493–502, https://doi.org/10.2475/ajs.259.7.493.
Holman, W.R., 1976, The origin of sheeting joints: A hypothesis [Ph.D. thesis]: Los Angeles, University of California at Los Angeles, 150 p.
Holzhausen, G.R., 1989, Origin of sheet structure, 1. Morphology and boundary conditions: Engineering Geology, v. 27, p. 225–278, https://doi.org/10.1016/0013-7952(89)90035-5.
Homberg, C., Hu, J.C., Angelier, J., Bergerat, F., and Lacombe, O., 1997, Characterization of stress perturbations near major fault zones: Insights from 2-D distinct-element numerical modelling and field studies (Jura mountains): Journal of Structural Geology, v. 19, p. 703–718, https://doi.org/10.1016/S0191-8141(96)00104-6.
Horowitz, D.H., 1982, Geometry and origin of large-scale deformation structures in some ancient wind-blown sand deposits: Sedimentology, v. 29, p. 155–180, https://doi.org/10.1111/j.1365-3091.1982.tb01717.x.
Howard, A.D., and Selby, M.J., 2009, Rock slopes, *in* Parsons, A.J., and Abrahams, A.D., eds., Geomorphology of Desert Environments (second edition): New York, Springer, p. 189–232, https://doi.org/10.1007/978-1-4020-5719-9_8.
Hunter, R.E., 1977, Basic styles of stratification in small aeolian dunes: Sedimentology, v. 24, p. 361–387, https://doi.org/10.1111/j.1365-3091.1977.tb00128.x.
Hunter, R.E., 1981, Stratification styles in eolian sandstones: Some Pennsylvanian to Jurassic examples from the western interior U.S.A., *in* Ethridge, F.G., and Flores, R.M., eds., Recent and Ancient Nonmarine Depositional Environments: Models for Exploration: Society of Economic Paleontologists and Mineralogists Special Publication 31, p. 315–329, https://doi.org/10.2110/pec.81.31.0315.
Jahns, R.H., 1943, Sheet structure in granites: Its origin and use as a measure of glacial erosion in New England: The Journal of Geology, v. 51, p. 71–98, https://doi.org/10.1086/625130.
Johnston, C.S., 1927, Polygonal weathering in igneous and sedimentary rocks: American Journal of Science, 5th series, v. 13, p. 440–444, https://doi.org/10.2475/ajs.s5-13.77.440.
Kocurek, G., and Dott, R.H., Jr., 1983, Jurassic paleogeography and paleoclimate of the central and southern Rocky Mountains region, *in* Reynolds, M.W., and Dolly, E.D., eds., Mesozoic Paleogeography of the West-Central United States (Rocky Mountain Paleogeography Symposium): Denver, Rocky Mountain Section, Society of Economic Paleontologists and Mineralogists, v. 2, p. 101–116.
Lazear, G., Karlstrom, K., Aslan, A., and Kelley, S., 2013, Denudation and flexural isostatic response of the Colorado Plateau and southern Rocky Mountain region since 10 Ma: Geosphere, v. 9, p. 792–814, https://doi.org/10.1130/GES00836.1.
LeGrand, H.E., 1949, Sheet structure, a major factor in the occurrence of groundwater in the granites of Georgia: Economic Geology and the Bulletin of the Society of Economic Geologists, v. 44, p. 110–118, https://doi.org/10.2113/gsecongeo.44.2.110.
Leith, K., Moore, J.R., Amann, F., and Loew, S., 2014a, In situ stress control on microcrack generation and macroscopic extensional fracture in exhuming bedrock: Journal of Geophysical Research: Solid Earth, v. 119, p. 594–615, https://doi.org/10.1002/2012JB009801.
Leith, K., Moore, J.R., Amann, F., and Loew, S., 2014b, Subglacial extensional fracture development and implications for Alpine Valley evolution: Journal of Geophysical Research: Earth Surface, v. 119, p. 62–81, https://doi.org/10.1002/2012JF002691.
Lemiszki, P.J., Landes, J.D., and Hatcher, R.D., 1994, Controls on hinge-parallel extension fracturing in single-layer tangential-longitudinal strain folds: Journal of Geophysical Research, v. 99, p. 22,027–22,041, https://doi.org/10.1029/94JB01853.
Levy, J.S., Marchant, D.R., and Head, J.W., 2010, Thermal contraction crack polygons on Mars: A synthesis from HiRISE, Phoenix, and terrestrial analog studies: Icarus, v. 206, p. 229–252, https://doi.org/10.1016/j.icarus.2009.09.005.
Loope, D.B., 2006, Dry-season tracks in dinosaur-triggered grainflows: Palaios, v. 21, p. 132–142, https://doi.org/10.2110/palo.2005.p05-55.
Loope, D.B., and Rowe, C.M., 2003, Long-lived pluvial episodes during deposition of the Navajo Sandstone: The Journal of Geology, v. 111, p. 223–232, https://doi.org/10.1086/345843.
Loope, D.B., Rowe, C.M., and Joeckel, R.M., 2001, Annual monsoon rains recorded by Jurassic dunes: Nature, v. 412, p. 64–66, https://doi.org/10.1038/35083554.
Loope, D.B., Seiler, W.M., Mason, J.A., and Chan, M.A., 2008, Wind scour of the Navajo Sandstone at the Wave (central Colorado Plateau, U.S.A.): The Journal of Geology, v. 116, p. 173–183, https://doi.org/10.1086/528902.
Loope, D.B., Kettler, R.M., and Weber, K.A., 2010, Follow the water: Connecting a CO_2 reservoir and bleached sandstone to iron-rich concretions in the Navajo Sandstone of south-central Utah, USA: Geology, v. 38, p. 999–1002, https://doi.org/10.1130/G31213.1.
Loope, D.B., Elder, J.F., and Sweeney, M.R., 2012, Downslope coarsening in aeolian grainflows of the Navajo Sandstone: Sedimentary Geology, v. 265–266, p. 156–162, https://doi.org/10.1016/j.sedgeo.2012.04.005.
Martel, S.J., 2006, Effect of topographic curvature on near-surface stresses and application to sheeting joints: Geophysical Research Letters, v. 33, L01308, https://doi.org/10.1029/2005GL024710.
Martel, S.J., 2011, Mechanics of curved surfaces, with application to surface-parallel cracks: Geophysical Research Letters, v. 38, L20303, https://doi.org/10.1029/2011GL049354.
Martel, S.J., 2017, Progress in understanding sheeting joints over the past two centuries: Journal of Structural Geology, v. 94, p. 68–86, https://doi.org/10.1016/j.jsg.2016.11.003.
Matthes, F.E., 1930, Geologic history of the Yosemite Valley: U.S. Geological Survey Professional Paper 160, 137 p.
McGill, G.E., 1986, The giant polygons of Utopia, northern Martian plains: Geophysical Research Letters, v. 13, p. 705–708, https://doi.org/10.1029/GL013i008p00705.
McGill, G.E., and Hills, L.S., 1992, Origin of giant Martian polygons: Journal of Geophysical Research, v. 97, p. 2633–2647, https://doi.org/10.1029/91JE02863.
Miller, D.J., and Dunne, T., 1996, Topographic perturbations of regional stress and consequent bedrock fracturing: Journal of Geophysical Research, v. 101, p. 25,523–25,536, https://doi.org/10.1029/96JB02531.
Mitchell, K.J., 2010, Factors contributing to the formation of sheeting joints: A study of sheeting joints on a dome in Yosemite National Park [M.S. thesis]: Honolulu, University of Hawaii at Manoa, 123 p.
Mollema, P.N., and Aydin, A., 1999, Fracture patterns and fault architecture in the East Kaibab monocline, *in* Close, J.C., and Casey, T.A., eds., Natural Fracture Systems in the Southern Rockies, 1999: Durango, Colorado, Four Corners Geological Society, p. 63–75.
Netoff, D.I., 1971, Polygonal jointing in sandstone near Boulder, Colorado: The Mountain Geologist, v. 8, p. 17–24.
Olson, J., and Pollard, D.D., 1989, Inferring paleostresses from natural fracture patterns: A new method: Geology, v. 17, p. 345–348, https://doi.org/10.1130/0091-7613(1989)017<0345:IPFNFP>2.3.CO;2.
Olson, J.E., Laubach, S.E., and Lander, R.E., 2009, Natural fracture characterization in tight gas sandstones: Integrating mechanics and diagenesis: American Association of Petroleum Geologists Bulletin, v. 93, p. 1535–1549, https://doi.org/10.1306/08110909100.
Parrish, J.T., Hasiotis, S.T., and Chan, M.A., 2017, Carbonate deposits in the Lower Jurassic Navajo Sandstone, southern Utah and northern Arizona: Journal of Sedimentary Research, v. 87, p. 740–762, https://doi.org/10.2110/jsr.2017.42.

Pollard, D.D., and Aydin, A., 1988, Progress in understanding jointing over the past century: Geological Society of America Bulletin, v. 100, p. 1181–1204, https://doi.org/10.1130/0016-7606(1988)100<1181:PIUJOT>2.3.CO;2.

Rawnsley, K.D., Rives, T., Petti, J.-P., Hencher, S.R., and Lumsden, A.C., 1992, Joint development in perturbed stress fields near faults: Journal of Structural Geology, v. 14, p. 939–951, https://doi.org/10.1016/0191-8141(92)90025-R.

Renshaw, C.E., and Pollard, D.D., 1994, Are large differential stresses required for straight fracture propagation paths?: Journal of Structural Geology, v. 16, p. 817–822, https://doi.org/10.1016/0191-8141(94)90147-3.

Riley, P., Murray, A.B., and Tikoff, B., 2012, Geometric scale invariance, genesis, and self-organization of polygonal fracture networks in granitic rocks: Journal of Structural Geology, v. 42, p. 34–48, https://doi.org/10.1016/j.jsg.2012.07.001.

Robinson, E.S., 1970, Mechanical disintegration of the Navajo Sandstone in Zion Canyon, Utah: Geological Society of America Bulletin, v. 81, p. 2799–2806, https://doi.org/10.1130/0016-7606(1970)81[2799:MDOTNS]2.0.CO;2.

Romani, J.R.V., and Twidale, C.R., 1999, Sheet fractures, other stress forms and some engineering applications: Geomorphology, v. 31, p. 13–27, https://doi.org/10.1016/S0169-555X(99)00070-7.

Sanderson, I.D., 1974, Sedimentary structures and their environmental significance in the Navajo Sandstone, San Rafael Swell, Utah: Brigham Young University Geology Studies, v. 21, p. 215–246.

Searls, M.L., and Phillips, R.J., 2007, Tectonics of Utopia Basin, Mars: Results from finite element loading models: Abstract 1965 presented at the 38th Lunar and Planetary Science Conference, League City, Texas, 12–16 March.

Seibert, N.M., and Kargel, J.S., 2001, Small-scale Martian polygonal terrain: Implications for liquid surface water: Geophysical Research Letters, v. 28, p. 899–902, https://doi.org/10.1029/2000GL012093.

Shabbir, G., Maqsood, A., and Majid, C.A., 2000, Thermophysical properties of consolidated porous rocks: Journal of Physics D: Applied Physics, v. 33, p. 658–661, https://doi.org/10.1088/0022-3727/33/6/311.

Shang, J., Hencher, S.R., and West, L.J., 2016, Tensile strength of geological discontinuities including incipient bedding, rock joints, and mineral veins: Rock Mechanics and Rock Engineering, v. 49, p. 4213–4225, https://doi.org/10.1007/s00603-016-1041-x.

Slim, M., Perron, J.T., Martel, S.J., and Singha, K., 2015, Topographic stress and rock fracture: A two-dimensional numerical model for arbitrary topography and preliminary comparison with borehole observations: Earth Surface Processes and Landforms, v. 40, p. 512–529, https://doi.org/10.1002/esp.3646.

St. Clair, J., Moon, S., Holbrook, W.S., Perron, J.T., Riebe, C.S., Martel, S.J., Carr, B., Harman, C., Singha, K., and Richter, D., 2015, Geophysical imaging reveals topographic stress control of bedrock weathering: Science, v. 350, p. 534–538, https://doi.org/10.1126/science.aab2210.

Stock, G.M., Martel, S.J., Collins, B.D., and Harp, E.L., 2012, Progressive failure of sheeted rock slopes: The 2009–2010 Rhombus Wall rock falls in Yosemite Valley, California, USA: Earth Surface Processes and Landforms, v. 37, p. 546–561, https://doi.org/10.1002/esp.3192.

Tuckwell, G.W., Lonergan, L., and Jolly, R.J.H., 2003, The control of stress history and flaw distribution on the evolution of polygonal fracture networks: Journal of Structural Geology, v. 25, p. 1241–1250, https://doi.org/10.1016/S0191-8141(02)00165-7.

Twidale, C.R., and Bourne, J.A., 2003, Active dislocations in the granitic terrains of the Gawler and Yilgarn cratons Australia, and some implications: South African Journal of Geology, v. 106, p. 71–84, https://doi.org/10.2113/1060071.

Twidale, C.R., and Bourne, J.A., 2009, On the origin of A-tents (pop-ups), sheet structures, and associated forms: Progress in Physical Geography, v. 33, p. 147–162, https://doi.org/10.1177/0309133309338660.

Williams, R., and Robinson, D., 1989, Origin and distribution of polygonal cracking of rock surfaces: Geografiska Annaler, Series A: Physical Geography, v. 71, p. 145–159, https://doi.org/10.1080/04353676.1989.11880283.

Wolf, R., 2010, Exfoliation of granite: https://www.flickr.com/photos/rwolf/4847904630/in/photostream/ (accessed April 2018).

Wong, I.G., and Humphrey, J.R., 1989, Contemporary seismicity, faulting, and the state of stress in the Colorado Plateau: Geological Society of America Bulletin, v. 101, p. 1127–1146, https://doi.org/10.1130/0016-7606(1989)101<1127:CSFATS>2.3.CO;2.

Yonkee, W.A., and Weil, A.B., 2015, Tectonic evolution of the Sevier and Laramide belts within the North American Cordillera orogenic system: Earth-Science Reviews, v. 150, p. 531–593, https://doi.org/10.1016/j.earscirev.2015.08.001.

Zahm, C.K., and Hennings, P.H., 2009, Complex fracture development related to stratigraphic architecture: Challenges for structural deformation prediction, Tensleep Sandstone at the Alcova anticline, Wyoming: American Association of Petroleum Geologists Bulletin, v. 93, p. 1427–1446, https://doi.org/10.1306/08040909110.

Zhao, J., Cai, J.G., Zhao, X.B., and Li, H.B., 2008, Dynamic model of fracture normal behaviour and application to prediction of stress wave attenuation across fractures: Rock Mechanics and Rock Engineering, v. 41, p. 671–693, https://doi.org/10.1007/s00603-006-0127-2.

Zoback, M.L., and Zoback, M.D., 1980, Faulting patterns in north-central Nevada and the strength of the crust: Journal of Geophysical Research, v. 85, p. 275–284, https://doi.org/10.1029/JB085iB01p00275.

Zoback, M.L., and Zoback, M.D., 1989, Tectonic stress field of the continental United States, *in* Pakiser, L.C., and Mooney, W.D., eds., Geophysical Framework of the Continental United States: Geological Society of America Memoir 172, p. 523–540, https://doi.org/10.1130/MEM172-p523.